MET.O.14

METEOROLOGICAL OFFICE
BOUNDARY LAYER RESEARCH BRANCH
TURBULENCE & DIFFUSION NOTE

T.D.N. No. 82

THE CARDINGTON TURBULENCE INSTRUMENTATION

BY

S. J. Caughey

February 1977

THE CARDINGTON TURBULENCE INSTRUMENTATION

BY

S. J. Caughey

Abstract:- An account is given of the instrumentation developed over the course of the last twenty years for the measurement of atmospheric turbulence from the tethering cable of a large (1300 m^3) captive balloon. Details are given of the design and performance of the various turbulence sensors employed and the associated electronic circuitry. The results of field evaluation studies carried out in the UK and the USA are outlined. Finally, some information on the data processing and analysis scheme is presented.

January 1977

CONTENTS

THE CARDINGTON TURBULENCE INSTRUMENTATION

1. Introduction

Our understanding of the structure of turbulence in the first few tens of metres of the atmosphere, both in stable and convective conditions, has progressed significantly in the last decade. However, a description of the characteristics of atmospheric turbulence throughout the depth of the boundary layer (typically about 1-2km deep in mid-latitudes over land) has not yet emerged, due to the very limited amount of data available for the rather inaccessible regions of the atmosphere. Highly accurate, fast response, turbulence sensors have been carried on aircraft (Lenschow, 1972), positioned on towers (Panofsky, 1973) and supported by the tethering cable of large balloons (Readings and Butler , 1972, Yokoyama, 1969). These systems have various advantages and disadvantages but perhaps the most powerful and flexible is the balloon based technique. This method alone offers the ability to make long term measurements of wind and temperature fluctuations, at many levels simultaneously, in the first few kilometers of the atmosphere, ie. in regions well above the reach of tall towers. Furthermore, the balloon system is easily transportable and thus can be used to investigate the effect of topography on turbulent flow. It is also much cheaper to maintain and operate than an aircraft. These general considerations have led to a gradual increase in the use of large tethered ballons in atmospheric research.

The purpose of this report is to outline the development of a package of instrumentation specifically designed to make accurate measurements of the turbulence field from the tethering cable of a large (1300 m^3) balloon. In the course of the last seven or eight years the equipment has been used to gather data which has greatly furthered the observational description of turbulence in the more inaccessible regions of the boundary layer. One of the first useful steps, provided by ascents with a single instrument package, was a demonstration of how the vertical distribution of small-scale turbulence in the first kilometer is related to the heating of the ground (Readings and Rayment, 1969.,

Rayment, 1973., Caughey and Rayment, 1974). Useful deductions were made from these measurements, in particular it was confirmed that in conditions with little or no surface heating the rate of generation of turbulent energy falls off rapidly from the surface. On the other hand with substantial heating of the surface the rate of generation is maintained throughout the whole mixed layer, by large scale convective motions. These early observations have also led to a useful generalization for convective conditions, in which the standard deviation of the vertical velocity is approximately proportional to the cube root of the product of height and heat flux (Caughey and Readings, 1974., Caughey and Readings, 1975).

The instrumentation has also been used to study the detailed structure of the interface at the top of the fair weather mixed layer. These observations have improved understanding of the entrainment mechanism at such an interface, in which air from the warm stable layer above is intermittently drawn into the cooler mixed layer and significantly contributes to the heat budget of that layer(Readings et.al.,1973 Rayment and Readings , 1974).

More recently a major boundary layer experiment has been carried out using the balloon-borne equipment in conjunction with the tower mounted US Air Force Cambridge Research Laboratories facilities over a very flat, sparsely populated, region of northwestern Minnesota (Readings et al 1974, Izumi and Caughey, 1976). The results from this experiment have considerably advanced our knowledge of the structure of atmospheric turbulence in convective conditions (Kaimal et al 1976., Caughey and Kaimal, 1977).

In the sections which follow the history of the probe development is outlined and evaluation studies of the system described. Full technical details of the present system are given, together with an outline of possible future developments.

2. History

The Cardington turbulence probe has been developed over a perid of years from an original instrument designed by Jones (1956). This device was constructed for use on the tethering cable of a kite balloon and measured vertical wind

fluctuations by means of a balsa-wood and tissue vane. An output voltage, directly proportional to the wind's inclination to the horizontal plane, was obtained by using the vane to operate a sliding contact on a wire potentiometer. This instrument also incorporated a 'windmill' type anemometer for speed measurements and arrangement for reference signals which served as a check on the functioning of the instrument and provided a calibration. These sensors were mounted on a vertically suspended arm with an air piston damper to counteract the varying angle of the balloon cable. In this prototype device all signals were relayed to the ground by cable and displayed on pen chart recorders.

Shortly afterwards a modified Ower (1949) airmeter (see Jones and Butler, 1958) was incorporated to permit the measurement of fluctuations in wind speed. This device gave four output pulses per revolution and these could either be counted over sequential periods or else converted to a pulse rate display. It was attached to the balloon cable on a mount that incorporated a wind sock to keep the sensor facing into wind. Also at about this time a thermistor was added to monitor air temperature and with only a few modifications (such as the use of a polyurethane foam vane and microtorque potentiometer) this system was used for several years.

During 1964 several major improvements were carried out, these were:-

(a) a sensitive platimum resistance temperature sensor was incorporated to measure high frequency temperature fluctuations (up to approx 11Hz in a wind speed of $5ms^{-1}$).

(b) the inclination vane was dispensed with and wind inclination to the horizontal plane was measured using a hot wire yawmeter, similar to that described by Jones (1961).

(c) a modified Casella electric contact cup anemometer was used to monitor wind speed fluctuations. This was similar to that described by Jones (1964) except that two brushes were used on a 15-sector commutator. At $5ms^{-1}$ wind speed the $\frac{1}{2}$ power frequency respone was about 0.5 Hz.

and (d) in order to provide the higher current requirement (especially of the hot wire yawmeter) lead acid batteries were used with a voltage stabiliser.

These batteries were housed in a box attached to the balloon cable a short distance below the turbulence instrument. Some of the associated electrical circuitry was housed in the tail fin on the probe.

Several alternative wind sensors were considered but it appeared that a cup anemometer was still the best overall device to use, especially if a minature type could be designed. Jones (1965) developed a standard size sensitive cup anemometer with photoelectric switching at 60 pulses per revolution enabling high resolution measurements of wind speed fluctuations. Using light weight expanded polystyrene cups a frequency response of around $1\frac{1}{2}$ Hz at 5 ms^{-1} was achieved. In 1968 this instrument was incorporated into the turbulence probe.

The damping system for the hot wire support underwent various changes but in 1969 the performance of a commercial miniature oil dashpot was evaluated. This proved very successful so this system (set for just sub-critical damping) has been used on all probes since then.

In order to resolve the longitudinal and lateral wind components the following modifications were made in 1973, (a) a second hot wire device (at right angles to the inclinometer) was added to sense the horizontal wind speed fluctuations (the sign convention adopted is that clockwise rotation of the wind vector is positive). And (b) a flux gate magnetometer was incorporated to sense the orientation of the probe vane with respect to the Earth's magnetic field. This flux value required a mounting which remained vertical so the front arm of the probe was improved by suspending it in a gimbal bearing with oil damping in two perpendicular planes.

More recently the cable telemetry (which presented handling difficulties) was replaced by radio transmission of data. In summary therefore the present version of the Cardington turbulence probe enables the measurement of the three orthogonal wind components and temperature. Full details of this instrument and associated equipment are given in the following section.

3. Description of the turbulence instrumentation

3.1 Mechanical details of the turbulence probe

The probe body is constructed from a tubular metal frame supporting a

a vertically suspended arm at the front with a vane at the other end to keep it directed into wind (see Plate (1)). A centrally located (at the point of balance) slotted bearing block, through which the balloon tethering cable passes, leaves the probe free to rotate in the horizontal plane. The bearing block rests on a platform clamped to the cable. When attached to a vertical support the position of the forward section of the probe is adjusted until the probe is in balance. A small oil damper is employed to prevent oscillations around the longitudinal axis of the probe.

Sensors are attached to the probe frame at mounting points and signals are led to circuitry in the fin of the vane and then by cable to a battery box positioned below the probe. The front arm of the vane, carrying the hot wire inclinometers and direction device, is maintained in a vertical position using gimbals and any balloon/cable induced motions are damped out by oil dampers acting in two orthogonal planes. A counterbalancing weight, with the same dimensions as the flux valve holder is attached to the other end on the suspended arm and is adjusted to initially set the arm vertical. Although various mechanical tests were carried out on the probe (eg to test its sensitivity to resonance oscillations), because of the complexity and the nature of the environment in which it was to operate, it was felt necessary to carry out a series of field trials to establish that the atmospheric variables were being properly measured. The results from these tests are fully described in section 4. A full set of workshop drawings of the probe and associated equipment are available (Ref No AO/12450).

3.3 The power supply and voltage regulator

The power supply consists of eight two volt (eight amp hour) lead acid cells housed in a box positioned a few feet below the probe. This battery box is also used as a junction box into which the probe is plugged and from which the output signals are fed to the transmitter. A compartment at the top of the battery box houses the voltage regulator and some circuitry associated with the direction device.

A voltage regulator is essential since the battery voltage varies with time

and temperature. The arrangement used gives a positive and negative voltage $\pm$ 6v balanced about earth - this balance being effected by adjusting the values of R5 and R6 (Diagram 1). The reference zener diode is selected to have near zero temperature coefficient ie at a nominal 5.6 V output. A further improvement is achieved by adjusting the current through it (using R2) so that the overall temperature coefficient is a minimum. The general specification of the voltage regulator is:-

Input	$14\frac{1}{2}$ to over 17V	
Output	$\pm$ 6V	
Line stability	($14\frac{1}{2}$ to 17V)	1 in 10,000
Load	" 0 to 450m A	1 in 2,500
Temperature coefficient		adjustable to better than 1 part in 50,000/°C

3.3 The temperature sensor and amplifier:-

This sensor consists of 180 cm of 25 micron diameter platinum wire wound non-inductively on a former prepared from clear acrylic plastic. During assembly the length of wire is adjusted so that its resistance falls as close as possible to a standard calibration value, so making all elements nominally the same. Tests carried out on these sensors (involving pulsing the current) have shown that for this diameter wire the time constant is 0.016 secs at 5 ms^{-1} decreasing to 0.014 secs at 10 ms^{-1}. A simple first order response calculation shows that the $\frac{1}{\sqrt{2}}$ frequency response (in a wind speed of 5 ms^{-1}) is about 11 Hz. This is supported by experimental temperature spectra.

In the design of any temperature sensor it is important to minimise the effects of wind velocity sensitvity. This topic has been considered in some detail by Wyngaard (1971) who expressed the velocity sensitivity coefficient of a resistance wire temperature sensor in terms of basic parameters. Following Wyngaard's formulation the velocity sensitivity coefficient of the present sensor was calculated to be about 5×10^{-6} °C sec cm^{-1} and this small value indicates that neither the derived temperature statistics nor their distributions are appreciably affected by the wind flow.

Signals from the temperature sensor are fed into a bridge circuit and amplifier, both of which are contained in the vane of the probe (see Diagram (2)). The reference arm (R_3) of the bridge is made of manganin wire (chosen for near zero temperature coefficient) - the total resistance of which is variable to accomodate centre zeroes other than 18°C, which corresponds to the 385 Ω value generally used. By varying the resistor R8 (connected to pins 1 or 5 of the MC1456) any temperature coefficient imbalance in the system can be corrected. There are also three resistances in the vane whose magnitudes correspond to the resistance changes in the sensor equivalent to changes of 3, 6 and 12°C in the air temperature. These are connected in series with the sensor (via switches) so that air temperatures other than 18°C may be positioned near mid scale with the bridge arm still near its nominal 385 Ω value. Resistors R1 and R2 in the bridge arm should be of high stability and matched for their temperature coefficients (a 2 ppm match corresponding to an accuracy in temperature measurement of about 0.01°C over a 20°C range).

All temperature sensors are accurately calibrated in an environmental chamber by immersing them in a stirred bath of white spirit and accuately noting resistance changes corresponding to small incremental temperature changes. For operational use each head amplifier is calibrated by substituting a decade resistance box for the temperature sensor and noting the output voltages for given resistances. The general specification of sensor and amplifier is as follows:

Frequency response	up to 11Hz at 5 ms^{-1}
Sensor sensitivity	1.4 ohms/°C
Amplifier output	± 3 v for ± 7°C
Amplifier zero settings	3°C steps from -3°C to + 18°C
" temperature coefficient, zero	.004°C/°C
" " " , range	.03%/°C

3.4 Wind speed sensor:

The sensor in use at present is a standard sized cup anemometer employing photoelectric switching with a 120 slot drum. This high switching rate is

necessary to give adquate resolution of wind speed fluctuations and also to minimize ripple at low wind speeds. Low inertia polystyrene cups (see Jones (1965)) are used to increase the overall frequency response of the sensor - wind tunnel tests have established that these cups have a time constant of .1 sec, which simple first order response theory gives a frequency of $1\frac{1}{2}$ Hz at the $\frac{1}{2}$ power level. All the circuitry associated with the photo-electric sensing is contained within the anemometer case (see Diagram (3)) and is adjusted to give a sine wave output symmetrical about earth. The output amplitude is set to 5 volts (peak to peak) using R4 and the circuit temperature coefficient minimized with R6. The output signal can either be transmitted to the ground directly as a frequency or converted to a dc voltage by a ratemeter housed in the battery box.

Diagram (4) shows the circuit diagram for the ratemeter. In this integrated circuit 1 converts the waveform from sinusoidal to square and introduces some hysteresis (adjustable with R2 and R3) to prevent false triggering (the level is set for $\pm$ 1V). Transistor 1 produces pulses of constant amplitude and width (about 20 μs) and also doubles the frequency. Integrated circuit 2 effects the frequency to voltage conversion which is biased to a zero of -3V by R9 and R10. Capacitor C3 should preferably be of polystyrene for stability and have a negative temperature coefficient, for compensation purposes. The gain is adjusted with R7 (metal foil) and R8 (high stability carbon). This combination provides the required amount of temperature compensation.

Each anemometer is calibrated in a wind tunnel by measuring its pulse rate against wind speed and each ratemeter is also calibrated by recording the output voltage for standard input frequencies. The general specification of the wind speed sensor is;

Response	up to $1\frac{1}{2}$ hz at 5 m sec^{-1}
Anemometer output	5v (peak to peak)
Ratemeter "	-3v to +3v for wind speed 0 to 18 m sec^{-1} (ie 0 to 1280 Hz)
" Linearity	$\pm$ .008% of full scale value.

Ratemeter temperature coefficient of zero	nil.
" temperature coefficient of scale	.002%/°C.

3.5 Wind inclination sensors:

Two hot wire devices are used, set at right angles, so that one records the inclination of the flow to the horizontal plane whilst the other gives the angle between the wind vector and the plane of the vane. Each element is made from 13μm diameter platinum wire arranged in a double 'V' geometry with sides 1cm long, so that each 'V' subtends an angle of 120 degrees and the two 'V''s are at eighty degrees to each other see Diagram (5)A. Using this double 'V' configuration the output remains linear even for deviations from the plane of the hot wire of up to $\pm$ 30 degrees. In the bridge circuit each arm of one 'V' is added in series to the corresponding arm of the other (see Diagram (5)B).

The bridge circuit is contained in the fin of the vane and measures the variations produced by the wind direction fluctuations. Resistors R1 and R2, through which the voltage is fed to the hot wire element, help to compensate for sensitivity variations due to wind speed.

During construction of the elements care must be taken to make the four arms precisely the same length with equal angles between them so that a near zero output is obtained in a steady wind flow normal to the sensor and with equal sensitivity for positive and negetive fluctuations. The elements are calibrated in a wind tunnel using a special holder which is adjustable so that each sensor may be set at various angles relative to the wind flow. Since the amplifier card used effects the overall calibration and it would obviously not be practical to calibrate specific heads with specific amplifiers the following system has been adopted; a calibrated test amplifier is used to obtain calibrations for all heads in the wind tunnel and then each probe amplifier is calibrated relative to the test amplifier prior to use in the field.

Because the hot wire head output varies quite markedly with wind speed corrections are applied to the sensor readings. This effect was thoroughly investigated in the wind tunnel by noting the variations in sensor output, at fixed inclinations to the flow, with windspeed. An average relation was

derived from the results for a set of sensors and expressed as a fourth order regression. $\phi_C=\phi_M\ (1.152-0.072V_T+0.0118V_T^2-0.000793V_T^3+0.0000204V_T^4)$ ϕ_C = corrected inclination, ϕ_M =measured value, V_T=total wind speed. This correction is applied automatically in the computer analysis scheme using the velocity values from the anemometer.

The time constant of 13μm diameter platimum wire has been estimated by Lander (MRP 873) as about 0.005 secs at 5 ms^{-1}. This implies a $\frac{1}{2}$ power level frequency response of 32 Hz. The general specification of the sensor/amplifier unit is as follows;

Response	32Hz at 5 ms^{-1}
Linear range	$\pm$ 40 degrees
Cross flow deviations for output variation $\pm$ 5%	$\pm$ 30 degrees
Amplifier output	$\pm$ 2V for $\pm$ 60 degrees
Variation of output with wind speed	Linear within $\pm$ 5% over the range 2 to 12 ms^{-1}
Amplifier temperature coefficient - of zero	.001 degrees/^{o}C.
Amplifier temperature coefficient - of scale	0.03%/^{o}C
Sensor power requirement	100mA at 10V.

3.6 The wind direction sensor:

Prior to the installation of this sensor in 1973 the probe could only resolve the vertical and total horizontal fluctuations in wind speed. By using a second hot wire sensor set at right angles to the inclinometer the fluctuations in horizontal wind could then be measured and it remained to devise a sensor to record the movement of the probe about the balloon cable. The device finally employed is a Sperry Thin Flux Valve (CT1) together with its normal resolver unit which detects the Earth's magnetic field (this is a substantially modified version of a prototype device developed at Porton Down). The reduced version (comprising basically of the flux valve, control transformer and electronic circuitry) conveniently fits onto the standard turbulence probe with the two circuit cards required positioned in the battery box. Power is supplied

from the normal ± 6V batteries and the consumption is about 100mA. The frequency response of the device was substantially improved by mechanical decoupling, however the disadvantages introduced were

(a) ambiguity outside a range of ± 90 degrees.

(b) a non linear output (near cosine).

The first of these factors causes little difficulty since the zero can be set for the expected mean wind direction and this is unlikely to change by more than ± 90 degrees over the course of a run. The effect of the second factor can also be minimized by setting the centre zero for each wind direction (adjustment can be made in steps of twenty degrees) so that during each run the most sensitive (and nearly linear) part of the response curve is being used.

In operation only the coil of the flux valve is used and this is mounted in a light weight holder at the top of the vertically suspended arm. A control transformer (Muirhead Type 26 V11CT4C) is housed in the lower holder where it is reasonably close to the flux valve and helps make up the suspended weight. The interconnection of units on the probe and in the battery box is shown in Diagram (6).

Two circuit cards are employed, one to generate the power supply and the other to decode the signal and provide a suitable output (see Diagrams (7) and (8) respectively). The specified drive for the flux valve is 23v at 400 Hz with a current requirement of 40mA. This is obtained by using a 400 Hz parallel - T oscillator feeding an ic audio power amplifier and an output transformer. In setting up the circuit R3 can be adjusted until the circuit oscillates reliably. A silicone diode (positioned close to the ic for thermal equality) is used to stabilise the output amplitude and is selected for low forward voltage since the input to the TBA641 component should be less than 1V (peak to peak).

In the power amplifier circuit (see Diagram (7)) R9 controls the gain and its value should be reduced until the final signal output reaches a maximum when it should be replaced by a fixed resistor close to but not greater than this value. This adjustment renders the flux valve output insensitive to power supply variations. The power amplifier is fitted with a heat sink of 22 sq cm

additional to that on the ic. Temperature variation effects in the oscillator/ power amplifier combination are compensated for by the thermistor TH1 wired so that it is in physical contact with the TBA 641 component. The 400 Hz output is also frequency doubled to act as a reference for the phase discriminator and a further tapping on the transformer is used to give a rectified 30V dc output to power the flux valve signal amplifier.

The second circuit card (see Diagram (8)) incorporates a signal amplifier, the output of which is tuned to 800 Hz by capacitance C22 and its gain is set with RV1 and R25 to give a maximum final output of $\pm$ 3V. This amplifier is followed by the phase discriminator to differentiate between a clockwise and anticlockwise movement of the probe from the arbitrary zero and then a voltage follower stage to give a low impedence output.

Since the overall unit is designed to sense the horizontal component of the Earth's magnetic field its sensitivity will of course depend on the local field strength. Furthermore the flux valve will also respond to any other magnetic field in the vicinity and care has to be taken that the Earth's magnetic field is not distorted by nearby objects. In practice it has been found that a reliable calibration may be obtained outdoors in an isolated area by erecting a screen around the apparatusto provide protection from the wind. An overall specification for the direction sensor is;

Range	$\pm$ 90 degrees with a near cosine response (near linear over the range $\pm$ 30 degrees)
Frequency response	up to 20 Hz
Output	$\pm$ 3v (adjustable to $\pm$ 5v)
Temperature coefficients,	
scale	.014%/^{o}C
zero	.0026 deg/^{o}C
Sensitivity to power supply variations,	
scale	.2%/V
zero	.004v/v

3.7 The radio telemetry system

All output signals from the turbulence probe are in the form of dc voltages ($\pm$ 3v) at low impedance and were originally relayed to the ground by lightweight multicore cable. Although cable is simple to use and causes practically no loss in signal accuracy it raises severe handling problems. For this reason a radio telemetry system has been adopted, which whilst increasing the flexibility of the system has also increased the complexity of operation and caused some degradation of the signal in transmission. An additional benefit however is that the multiplexed signals from a particular turbulence probe may be recorded directly on a single track of a multitrack tape recorder

The transmitter package (manufactured by Dynatel Ltd., now part of EMI Ltd) is attached to the balloon cable a short distance below the probe/battery box pair. It contains up to ten voltage controlled oscillators (VCO's) which convert the probe voltage signals to frequencies. These are then multiplexed in a mixer and fed to a crystal controlled, frequency modulated, transmitter operating in the 400-410 MHz band. During evaluation tests it was found that the stability of VCO's depended on temperature and power supply voltage. Thus in order to improve accuracy a power supply regulator (derived from the transmitter power supply) was incorporated and each VCO periodically calibrated against temperature. When in operation the temperature of the VCO's in the transmitter package is monitored so that corrections may be applied at the analysis stage. With these included the overall accuracy of the system is better than 0.1%.

At the surface the transmission is received by a directional antenna (incorporating a head amplifier) and is then fed through low loss coaxial cable to a crystal controlled receiver (Dynatel DRT-1). Here the carrier frequency is removed and a reference frequency added which can subsequently be used for compensation if the multiplexed signal is tape recorded before later being decoded and reproduced. Discriminators are used to convert the frequencies to dc voltages so reproducing the original signals. Provided the discriminators are allowed to reach an 'equilibrium' temperature (ie not switched on and off)

the drift in the output is small, of order .006% hr^{-1} at worst. This means that across typical recording periods of several hours the overall accuracy of the radio transmission system is about 0.1%.

By recording the multiplex signal directly on magnetic tape the flexibility of the system is increased since the final data output form can be chosen at a later date. At Cardington two output forms are normally used,

(i) digitisation by mini computer and storage on further magnetic tapes.

(ii) digitisation and logging directly on 5h paper tape. A further important advantage of directly recording the multiplexed signal is that it removes the need for 'on the day' calibration of the discriminators, since these are only used for diagnostic purposes.

4. Evaluation of the system

4.1 The performance of the probe on a fixed support

Although various tests were carried out in the laboratory and in a wind tunnel, the complexities of the complete system and the nature of the environment in which it had to operate meant that a series of field trails were necessary to ensure that the atmospheric variables were being measured correctly. A first step in this evaluation was the comparison of the performances of two three component probes ie (T, Ø and V) mounted on fixed supports at a height of 8.5 metres and set about 2 metres apart. These experiments were conducted during 1970 at Cardington. Each 'run' lasted one hour, during each of these the boom, on which the probes were mounted, was approximately perpendicular to the mean wind direction. The analogue voltages were sampled once a second and the variables punched on paper tapes which were subsequently processed on a Ferranti Mercury computer. Fluctuations were measured with respect to the linear regression over each hour.

Unfortunately many of the quantities of interest are sensitive to slight rotations of the frame of reference (see Rayment and Readings, 1971). Thus as the axes of these probes cannot be determined with sufficient accuracy from instrumental techniques alone, it was decided to fix them by assuming that the

mean vertical wind speed ($\bar{w}$) was zero during each run.

The results of these tests are summarised in Figs (9) and (10), which show the comparison between the statistics σ_T, σ_{u_H}, $\overline{u_H'W'}$ and $\overline{W'T'}$ from two probes. It can be seen that, apart from a slight tendency for Probe 8 to record larger values of $\overline{u_H'W'}$ than Probe 7, the two sets of values are in close agreement. A more detailed analysis, based on the 20-min averages, confirmed this impression (see Table (1) and Readings and Butler (1972)). It was also found that the mean wind speeds agreed within a few cms sec^{-1} and that the temperature differences were reproducible to within a few hundredths of a degree (^{o}C). Although some of these differences (notably between the fluxes) are slightly larger than might have been expected, the complexities of the overall operating system mean that it would be unwise to conclude that the discrepancies are purely atmospheric in origin. However it seems fair to state that the various quantities can be measured, on a fixed support, to at least the accuracies implied by Table (1).

An earlier series of comparison tests took place in Boston, Mass. in the autumn of 1969, when a three-component Cardington probe (ie T, Ø and V) was compared with a three-component (u, v and w) sonic anemometer operated by the Air Force Cambridge Research Laboratories (Readings and Butler, 1969 Haugen et al 1971, Kaimal et al 1974). The instruments were mounted on fixed supports on the top of a 15.5 metre tower and each run lasted for about ten minutes. Owing to obstructions around the site runs could only be done when the wind was westerly and this somewhat limited the data available for comparison purposes. The analogue signals from the instrumentation were sampled at 20 Hz and processed in real time.

The definition $\bar{W}$=o was again used to determine the reference axes for the Cardington probe but the sonic anemometers were lined up using purely instrumental techniques. Thus the two sets of values are not entirely comparable, although the difference was found to be small. A further difficulty arose from the Cardington probe measuring u_H (the total horizontal wind speed) whilst the sonic anemometers.

difference was small (see Haugen et al (1975)). An additional possible complication could have been the relatively slow response of the cup anemometer which would have caused the Cardington probe to underestimate $\overline{u_H'W'}$ and σ_{u_H} if there had been any significant high frequency contributions to these quantities at a height of 15.5 metres.

The results of these experiments are summarised in Figs (11) and (12) and it can be seen that the two sets of data are in quite close agreement, despite the points discussed above. In fact the level of agreement is comparable with that observed during the interprobe comparison described earlier. Furthermore, on the few occasions when a second sonic anemometer was available the correlation between the two sonics was slightly less than that between the Cardington probe and each of them individually.

4.2 The Effects of balloon movement

The experiments described in the previous section have shown that the probe can be successfully operated on a fixed support but it does not necessarily follow that it will perform equally well when mounted on the balloon tethering cable, which is in a state of continuous motion. In certain conditions, such as strong winds and intense thermal activity, these movements can be quite large and rapid so there is a real possibility that they may introduce spurious contributions to some of the measured turbulence variables. Since there is no well established theoretical framework with which to predict the likely effects recourse was made to an experimental investigation of the problem.

One of the first setps in this study was to use theodolites to monitor the movements of the balloon cable. Although in many respects the results were rather inconclusive, they did confirm that the predominant mode of motion was a series of lateral oscillations across the mean wind direction and that the problem was serious enough to merit further detailed investigation (Readings and Thompson, 1974). Thus in 1971 a series of comparison experiments were carried out at Fort Eglin Air Force Base, Florida (see Haugen et al 1975). During these the performances of two three-component probes (ie V, ϕ and T) were compared with

those of three-component sonic anemometers. The Cardington probes were attached to the balloon tethering cable at heights of 150 and 300 metres and the sonic anemometers were mounted at the same heights on a 370m tower comparison periods being limited to occasions when the wind was blowing from the balloon to the tower. Four theodolites were used to monitor the motions of the balloon-borne probes and all data was recorded in digital form on magnetic tape.

At the time of these experiments the MRU probe did not resolve the horizontal wind components but instead measured the total horizontal wind speed u_H. The sonic anemometer data, on the other hand, were analysed to provide the magnitude of the horizontal wind speed along the mean direction from the 1 hour run periods. It can be shown that the fractional difference between these two quantitites is of order $\overline{v^2}/\overline{u^2}$ where v is the fluctuating component in the lateral direction and this seldom exceeds a few percent in typical steady state conditions. Thus throughout the rest of this comparison the difference is ignored: the AFCRL data were processed to give U's and the MRU to give H_H's.

The most important factor in the comparison of the 1h statistics was found to be the wind direction relative to the line connecting the balloon tethering point with the tower. Examination of the classified data showed that good agreement was obtained only when this angle was $\leqslant 15^\circ$. This is consistent with the current view that the predominant scales of motion in the lower boundary layer are much smaller in the lateral than in the streamwise direction (Lumley and Panofsky, 1964). Hence a useful comparsion of the two techniques is possible only when the spatial sparations and wind azimuth deviations are small enough to ensure that both sensors are imbedded in the same flow field. The nine runs selected for this study were subjected to spectral and cospectral analyses (for details of the computational scheme see Kaimal et al 1972). Differences in spectral estimates for like variables were also computed to investigate specific sources of error and natural frequencies inherent in each technique.

A comparison of the mean horizontal wind U from the balloon probe and the tower (see Diagram 3) shows good correlation, which is encouraging in view of the

of the fact that the balloon and the probes attached to its cable were constantly in motion. The predominant mode of motion for a captive balloon of this design is a lateral oscillation. Oscillations in the vertical and streamwise directions are also present but these arise primarily from the constraints imposed by the tethering cable and buoyancy. Clearly then a predominantly lateral balloon movement will result in an overestimation of the mean horizontal wind speed and since the lateral velocity increases with increasing height above the tethering point, one would expect the overestimation to be less at 500 ft than 1000 ft. The distribution of points in Fig (13) shows this to be the case, with about 7% and 11% overestimates for these two heights respectively. Analysis of the double theodolite data showed that the average ratio of the standard deviations of the lateral motions (σ_L), at these two heights, was 0.7. This in fair agreement with the ratio of the U discrepancies, ie 7/11 $\sim$ 0.6. Hence it would seem that the primary reason for the balloon-borne probe overestimation of horizontal wind speed is due to the lateral component of balloon motion.

The comparison of the variances and covariances involving U, W and T are given in Figs (14) and (15). The former shows that the balloon-borne measurements overestimates σ_U^2 by about 15% at 500 ft and about 30 % at 1000 ft. The ratio of the square root of these two values ($\sim$0.7) is close to the ratio of the σ_L's and in line with the mean wind speed comparisons the σ_U^2 differences increase with increasing σ_L. Fig (14) also indicates some systematic differences between the variances σ_W^2 and σ_T^2 from balloon and tower, with these two quantities being underestimated by the balloon instrumentation by about 10% and 5% respectively. However, neither of these differences shows any relation to probe height or balloon motion. It is felt that they may be due to small calibration shifts in the MRU or AFCRL sensors, however it is possible that in the σ_W^2 case strong convective updrafts and downdrafts were underestimated by the MRU hot wire inclinometer.

Perhaps the best example of agreement between the two techniques is found in the covariance of U and W (see Fig (15)). This is particularly encouraging

since $\overline{UW}$ is one of the most difficult quantities to measure in the surface layer. Covariances of U and T agree well at moderate and low values but show some scatter at larger values. However there was no clear relation between any of these differences and the measures of balloon motion.

For the covariance of W and T reasonable agreement is found in all except the highest covariance values (ie $\overline{WT} \sim 0.15$ m $^{\circ}$C s^{-1}) at 500 ft, which are underestimated by the balloon-borne equipment. Possible explanations, as with the σ_W^2 and σ_T^2 comparisons, include calibration shifts and possible underestimates of vertical air motion due to vertical displacements of the sensor in strong convective conditions.

A more detailed comparison of the two techniques can be obtained through spectral and cospectral analyses. The horizontal wind speed spectral levels $n\,S_u(n)$ (Fig (16)) show the expectedly larger values from the balloon-borne sensors than those from the tower, but the most notable increase in variance is in the 0.1 to 1.0 Hz band where the only natural frequency of significance is that of the vane and arm assembly (0.3 Hz), supporting the sensors. The natural period of the balloon motion is of the order of a minute, which is too long to be the direct cause of the overestimation at such a high frequency. It is not clear at the present time how energy is transferred from the frequencies associated with the balloon cable motions to those corresponding to the vane's natural period.

The W spectrum (see Fig 16)) shows somewhat reduced spectral levels from the balloon-borne probe at low and mid-frequencies, but merges in with the tower spectrum above about 1.0 Hz. The general characteristics of the two spectra are remarkably alike and this implies that the two instruments were in essentially the same turbulence field. Similar comments apply to the temperature spectra in Fig 16., although the difference between the observed intensity levels in this case is much smaller.

The cospectra (see Fig (17)) reflect the good agreement already noted in the covariance data. The WT and UW spectra both exhibit a peak at about .002 Hz, which is too far removed from the frequencies associated with balloon movement to

be seriously affected by it.

These analyses of data gathered from balloon-borne and tower-based sensors indicate that several important parameters in the planetary boundary layer can be measured without serious error due to wind induced motions of the balloon and its tethering cable. Vertical momentum flux, horizontal heat flux and vertical heat flux compare quite well. The quantities most severely affected by balloon/cable motions are the mean and variance of the horizontal wind speed. These errors are quite well correlated with σ_L and very probably reflect the apparent lateral wind component, an effect which could be reduced by increasing the balloon-probe separation.

5. Concluding Remarks

There are several significant improvements to the Cardington turbulence instrumentation, as described in this paper, which are in the process of being implemented. Several alternative temperature sensors have recently been built which permit operation in cloud and fog (although with reduced frequency response) and near the surface, where the turbulence length scales are small. A miniature anemometer (rotor dimension $\sim$4 cms) has also been tested and shown to provide a significant improvement on the performance of the relatively slow response cup anemometer. This should also facilate near surface operation of the probe, especially in stable conditions.

In the near future it is planned to add a humidity device to the range of probe sensors, to investigate the characteristics of humidity fluctuations in similar studies to those already carried out for heat flux and momentum. A further useful addition to the balloon-borne equipment will be an accurate pressure sensor to record the heights of the packages, without recourse to double theodolite measurements. These modifications and additions to the present system should significantly improve its flexibility and operating range.

Appendix 1. Definition of the probe analysis axes

Consider the probe orientation in the horizontal plane as shown in Fig 18, with V_H indicating the direction of the instantaneous horizontal wind. The sign convention adopted is that all clockwise rotations are considered positive. The angle Θ_H is the projection of the measured angle Θ (ie the angle between the wind vector and the plane of the vane) on the horizontal plane. If ϕ is the measured angle between the wind vector and the local horizontal then it can be easily shown that,

$$\Theta_H = \sin^{-1}\left[\frac{\sin\Theta}{\cos\phi}\right]. \qquad (1)$$

In practice however the Θ and ϕ sensors cannot be set by instrumental techniques accurately enough to ensure near zero output for zero values of the parameters. To overcome this problem it is assumed that the mean values of these are zero over some fairly long period of time ie the quantities $\overline{\phi'}$, $\overline{\Theta'}$ are set to zero,

$$\Theta' = \Theta - \overline{\Theta}$$
$$\phi' = \phi - \overline{\phi}$$

thus equation (1) becomes

$$\Theta_H = \sin^{-1}\left[\frac{\sin\Theta'}{\cos\phi'}\right] \qquad (2)$$

In physical terms the assumption that $\overline{\Theta} = 0$ amounts to the expection that, on average, the mean vane direction corresponds to the mean horizontal wind direction (ie $\overline{\Theta}_H \approx 0$). This assumption also means that the longitudinal wind (U) direction is given by $D_{ref} + \bar{D}$ (in degrees from magnetic North). The inclination assumption ie that $\overline{\phi} = 0$, or that the mean inclination of the flow over a long period of time is zero, is also reasonable, though it should be noted that this is not quite equivalent to the assumption that the mean vertical velocity is zero. The averaging period for which this is a meaningful procedure varies both with height and stability eg in the higher regions of the convective boundary layer variations in ϕ with a time scale of 15-20 minutes are common (especially in light winds) and averages over periods of at least $1\frac{1}{2}$ h are required.

The angle D' in Figure 17 is the difference between the vane direction and the mean longitudinal wind direction (note that with this particular orientation

of probe and wind vector D' is a negative angle). If V_T is the magitude of the total wind vector then it follows that

$$V_H = V_T \cos \phi'$$

and hence the expressions for the three orthogonal components of V_T are

$$U = V_T \cos \phi' \cos (D' + \Theta_H), \quad V = -V_T \cos \phi' \sin (D' + \Theta_H), \quad W = V_T \sin \phi \qquad (2)$$

Appendix 2 Production of overall calibration constants

The transmission system consists of a set of linked but independent linear systems. An equation for the i^{th} stage can be written

$$O = \frac{Ii}{mi} + Ci$$

where O_i = the output from the i^{th} stage and the input to the $i + 1^{th}$ stage.

I_i = the input to the i^{th} stage

m_i = the linear stage can

and C_i = the zero offset.

For an r stage system the input at the first stage ie the meteorological parameter is,

$$I_1 = m_1 m_2 \cdots m_r \left[O_r - \left(C_r - \frac{C_{r-1}}{m_r} + \cdots + \cdots \frac{C_1}{m_2 m_3 \cdots m_r} \right) \right]$$

and can be written as

$$I_1 = SF(O_r - ZO)$$

where O_r is the final output and SF, ZO are the overall scale factor and zero respectively

Appendix 3 Outline of the data processing scheme

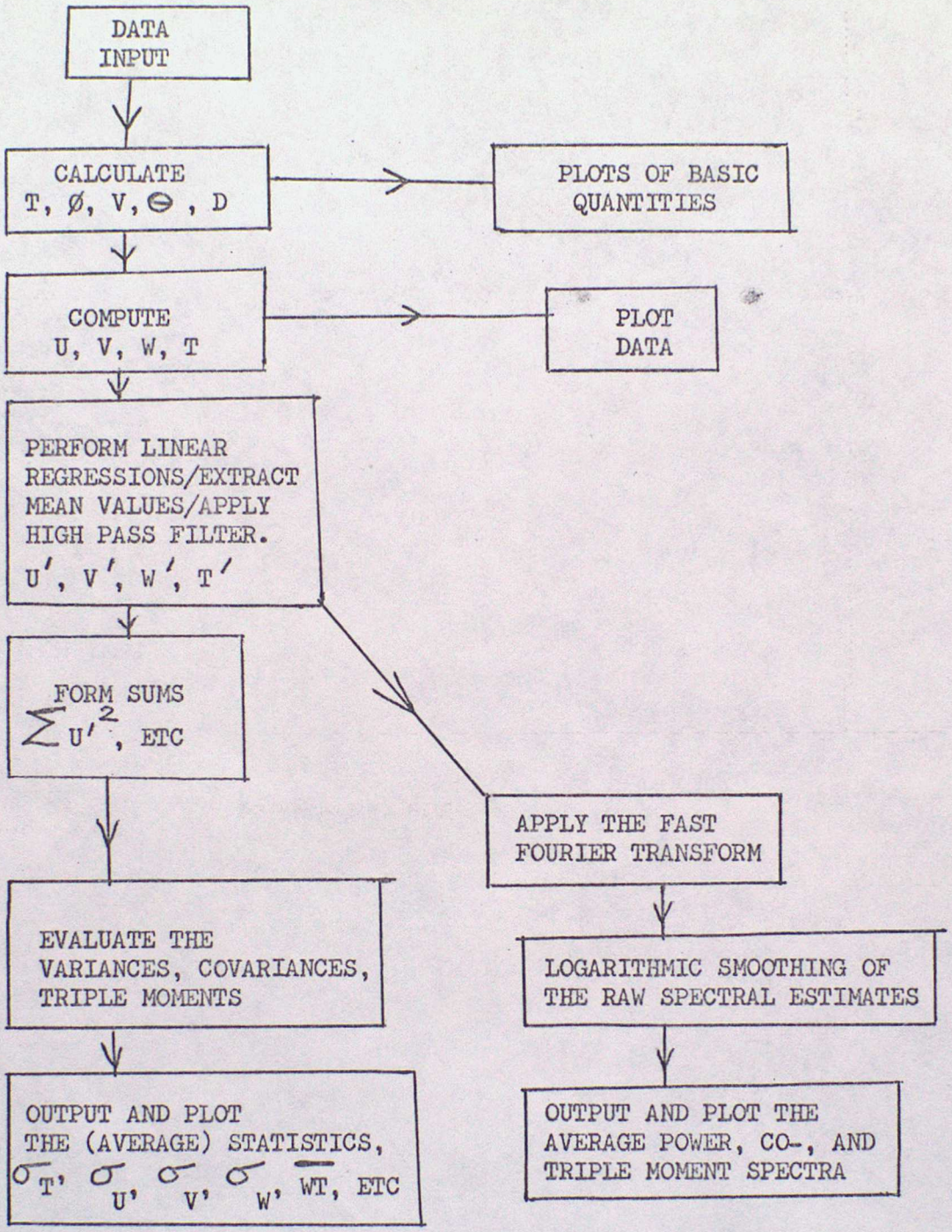

List of References

Caughey, S J and Rayment, R 1974 'High Frequency Temperature Fluctuations in the atmospheric boundary layer' Boundary layer Met 5, 489-503.

Caughey, S J and Readings, C J 1974 'The Vertical Component of turbulence in convective conditions' Advances in Geophysics, Vol 18A, 125-130.

Caughey S J, and C J Readings 1975 'An Observation of Waves and Turbulence in the Earth's Boundary Layer' Bound Layer Met 9, 279-296.

Caughey, S J and Kaimal, J C 1977 'Vertical Heat Flux in the convective boundary layer'. To be published.

Haugen D A, Kaimal J C and E F Bradley 1971 'An Experimental study of Reynolds Stress and heat flux in the atmospheric surface layer' Quart J Roy Met Soc 97, 168-180.

Haugen D A, Kaimal, J C Readings, C J and R Rayment 1975 'A Comparison of balloon - borne and tower - mounted instrumentation for probing the atmospheric surface layer'. J Appl Meteorology, 14, 540-545.

Izumi, Y and S J Caughey 1976 'Minnesota 1973 atmospheric boundary layer experiment data report'. AFCRL Environmental Research Paper No 547.

Jones, J I P 1956 'A vertical gustiness recorder for use with a captive balloon' Porton Technical Paper No 536.

Jones, J I P and H E Butler 1958 'The measurement of gustiness in the

first few thousand feet of the atmosphere'.
Quart JR Met Soc 84, pp 17-24

Jones, J I P 1961 'The Measurement of turbulence near the ground'
Porton Technical Paper No 786.

Jones, J I P 1964 'Continuous computation of the standard deviations of longitudinal and lateral wind velocity component'
Brit J of Appl Physics 15, pp 467-480.

Jones, J I P 1965 'A portable sensitive anemometer with proportional DC output and a matching wind velocity component resolver'.
J Sci Instruments.

Kaimal, J C, Wyngaard J C Haugen D A, Cote, O R Izumi, Y, Caughey S J and Readings, C J 1976 'Turbulence Structure in the Convective Boundary Layer'
J.Atmos. Sci. 33,
2152-2169

Kaimal, J C, Newman, J T Bisberg, A and Cole, K 1974 'An Improved Three - Component Sonic Anemometer for investigation of atmospheric turbulence'
Instrumental Society of America publication 'Flow its Measurement and Control in Science and Industry'
pp 349-359.

Kaimal, J C, Wyngaard, J C, Izumi Y and O R Cote 1972 'Spectral Characteristics of surface layer turbulence
Quart JR Met Soc 98, 563-589.

Lenschow D H 1972 'The Measurement of Air Velocity and Temperature using the NCAR Buffalo, Aircraft Measuring System'

NCAR Technical Note EDD-74, Boulder, Colorado pp 39.

Ower, E 1949 'The Measurement of air flow' London (Chapman and Hall) pp 150.

Panofsky, H A 1973 'Tower Micrometeorology' in 'Workshop on Micrometeorology' published by the American Meteorological Society. Editor, D A Haugen.

Rayment, R 1973 'An Observational Study of the high frequency fluctuations of the wind in the Atmospheric Boundary Layer' Boundary - Layer Meteorology 3, 284-300.

Rayment, R and C J Readings 1971 'The Importance of Instrumental Tilt on measurements of atmsopheric turbulence' Quart JR Met Soc, 97, pp 124-130

Rayment, R and C J Readings 1941 "A case study of the structure and energetics of an inversion". Quart J R Met Soc. 100, pp 221-233.

Readings, C J and R Rayment 1969 'The high-frequency fluctuation of the wind in the first kilometer of the atmosphere' Radio Science 4 pp 1127-1131

Readings C J and H E Butler 1969 'The 1969 comparison of AFCRL and Cardington Turbulence sensors' Unpublished Met Office Turbulence and Diffusion Note No 8.

Readings C J and H E Butler 1972 'The Measurement of atmospheric burbulence from a captive balloon' Met Mag 101, 286-298

Readings, C J and N Thompson 1974 'The Movement of a tethered kite balloon and its cable'. Unpublished Met Office Turbulence and Diffusion Note No 52.

Readings, C J and Haugen, D A 1974 'The 1973 Minnesota atmospheric boundary layer experiment'. Weather, 29, 309-312.

Readings, C J., E Golton and K A Browning 1973 "Fine scale structure and mixing within an inversion". Bound. Layer Meteorol. 4, 275-287.

Wyngarrd, J C 1971 'The effect of velocity sensitivity on temperature derivative statistics in isotropic turbulence'. J Fluid Mech 48, 763-796.

Yokoyama, O 1969 'Measurements of wind fluctuations by a vane mounted on a captive balloon cable' J Met Soc Japan 156-166

List of Figures

TABLE 1

The accuracies implied by the comparison runs on fixed supports (using 20 minute averages).

Quantity	Mean difference $\pm$ standard error
σ_T	0.006 $\pm$ .001 (^oC)
σ_{U_H}	0.0 $\pm$ .3 (cm sec^{-1})
σ_W	-1.7 $\pm$ .3 (cm sec^{-1})
$\overline{U'_H W'}$	9 $\pm$ 2 (per cent)
$\overline{W'\theta'}$	8 $\pm$ 2 (per cent)

The 1974 Cardington Probe

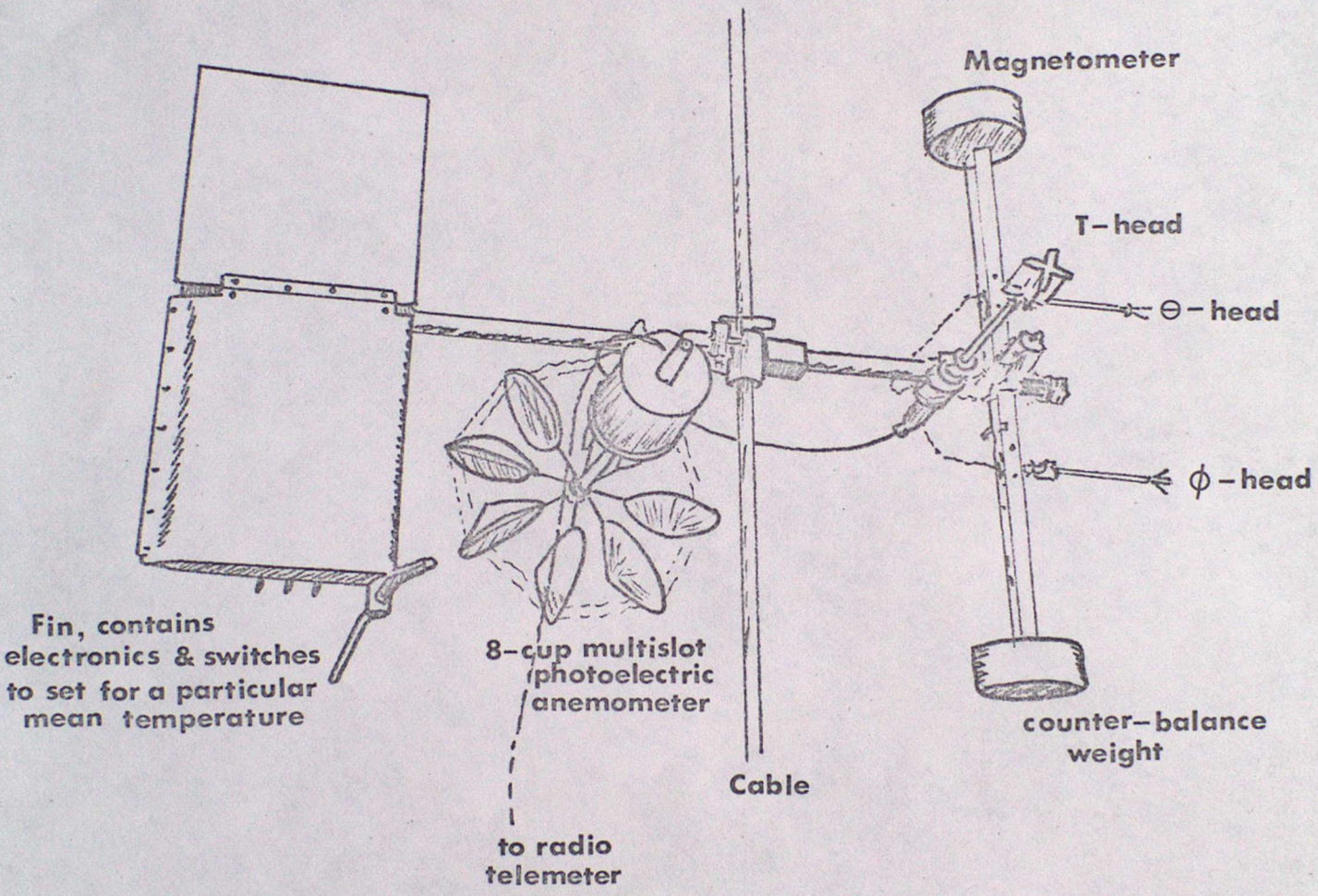

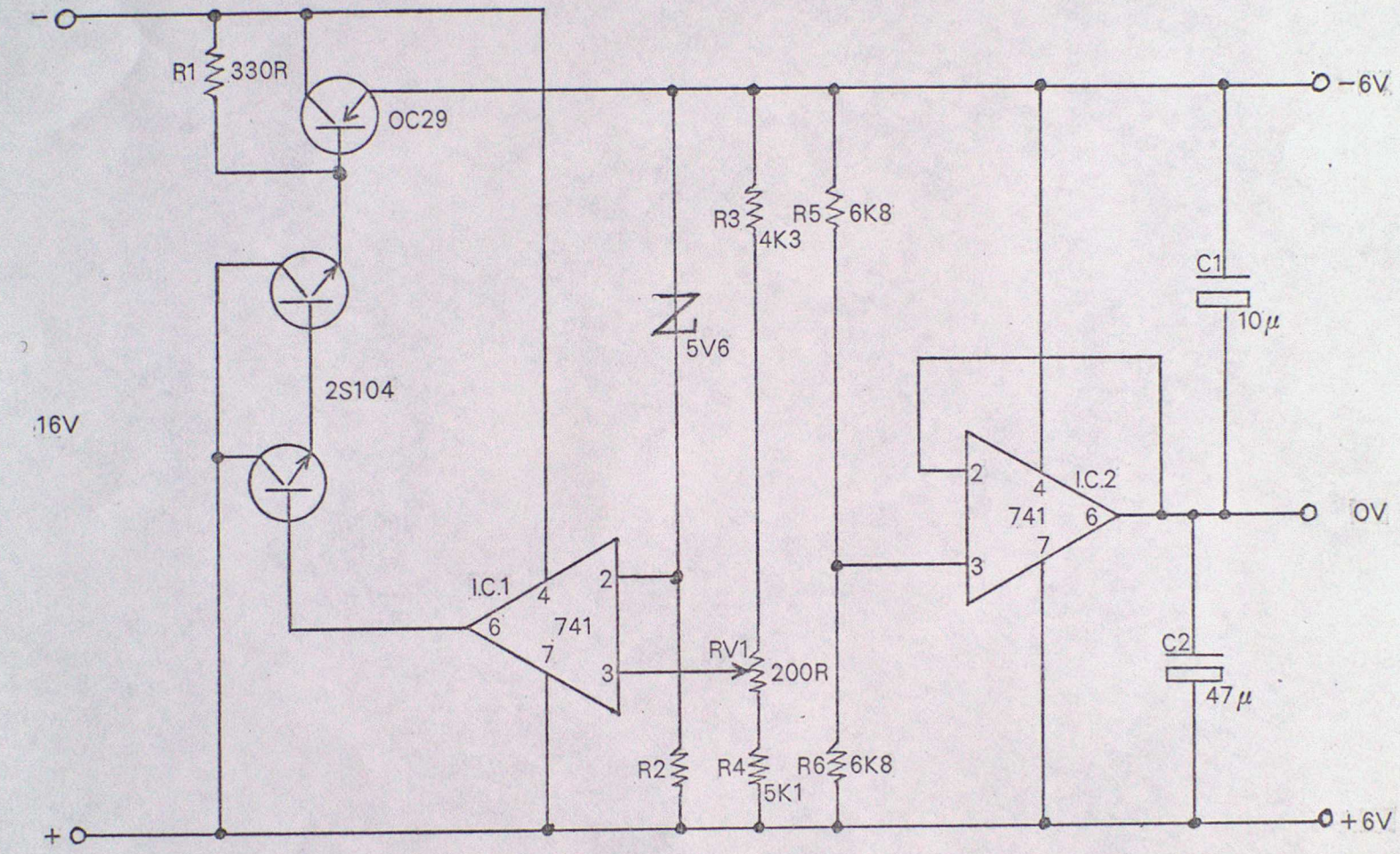
−
R1 330R
OC29
2S104
16V
+
R3 4K3
R5 6K8
5V6
−6V
C1
10μ
I.C.1
741
I.C.2
741
RV1 200R
R2
R4 5K1
R6 6K8
C2
47μ
0V
+6V

DIAGRAM 1.

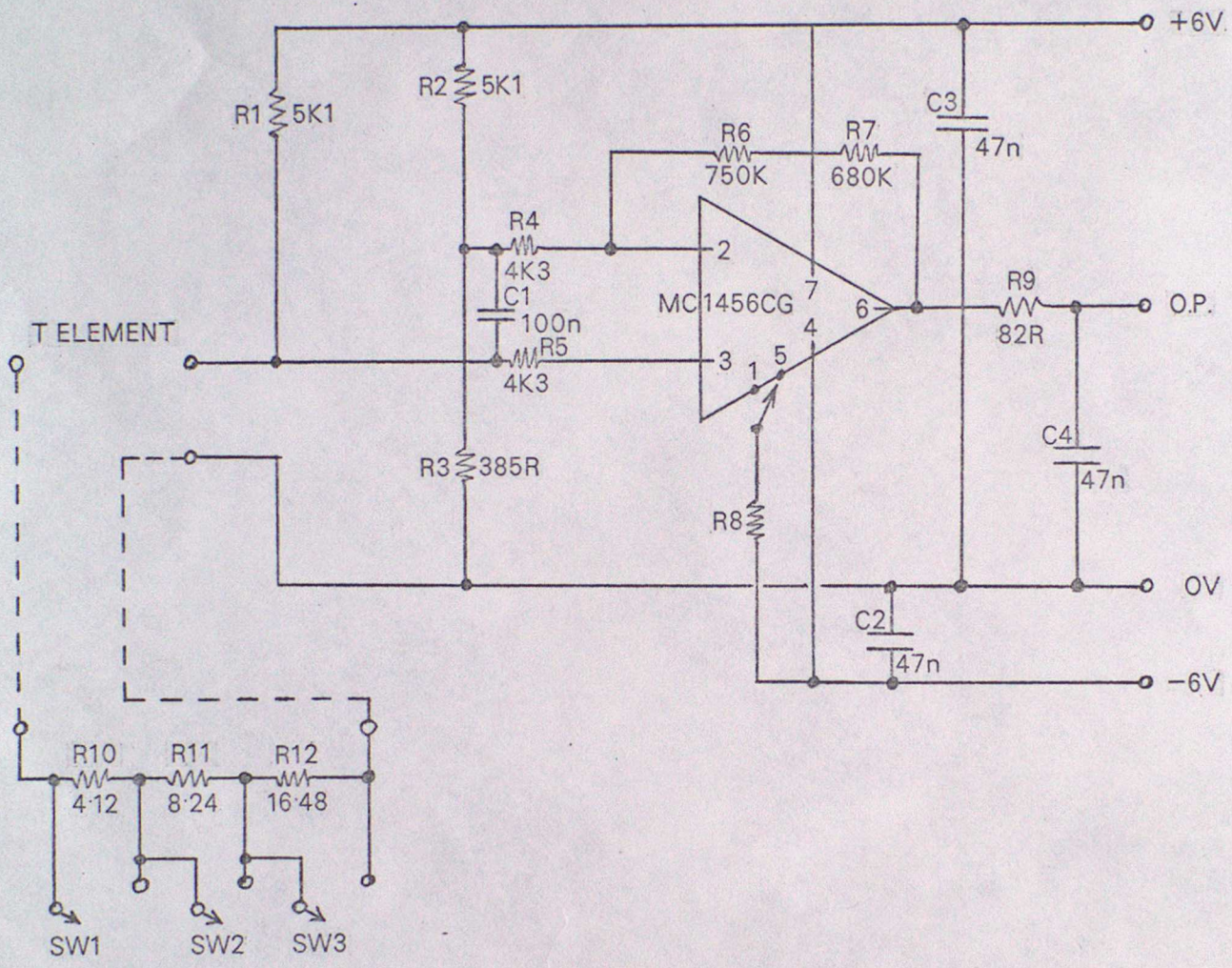

ZERO SET SWITCHES.

DIAGRAM 2.

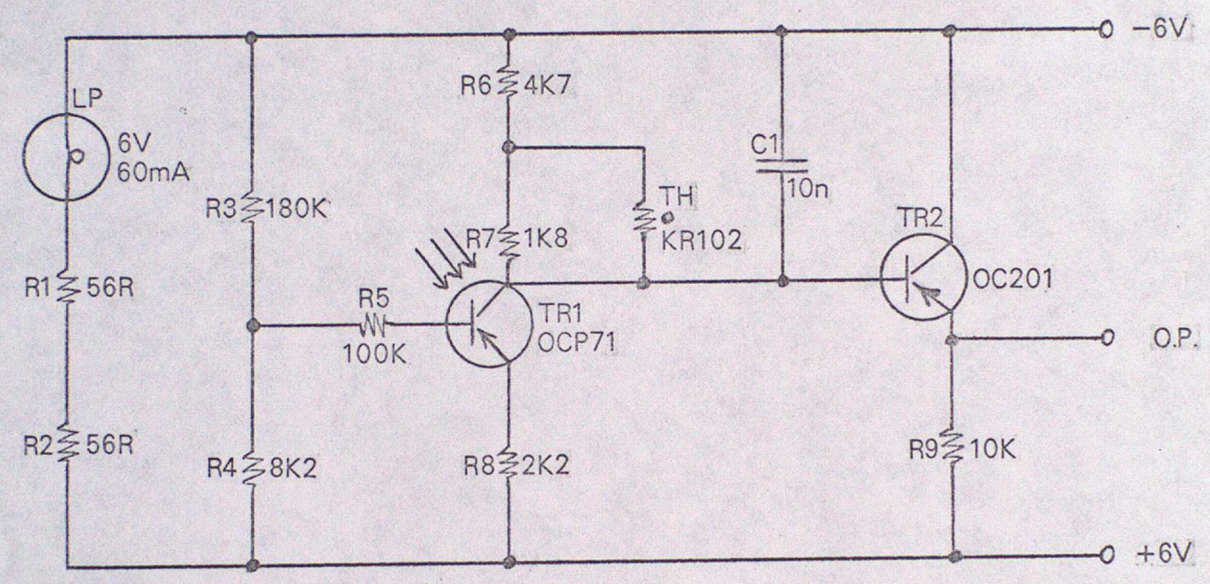
-6V
LP
6V
60mA
R6 4K7
C1
10n
TH
KR102
R3 180K
R7 1K8
TR2
OC201
R1 56R
R5
100K
TR1
OCP71
O.P.
R2 56R
R4 8K2
R8 2K2
R9 10K
+6V

DIAGRAM 3.

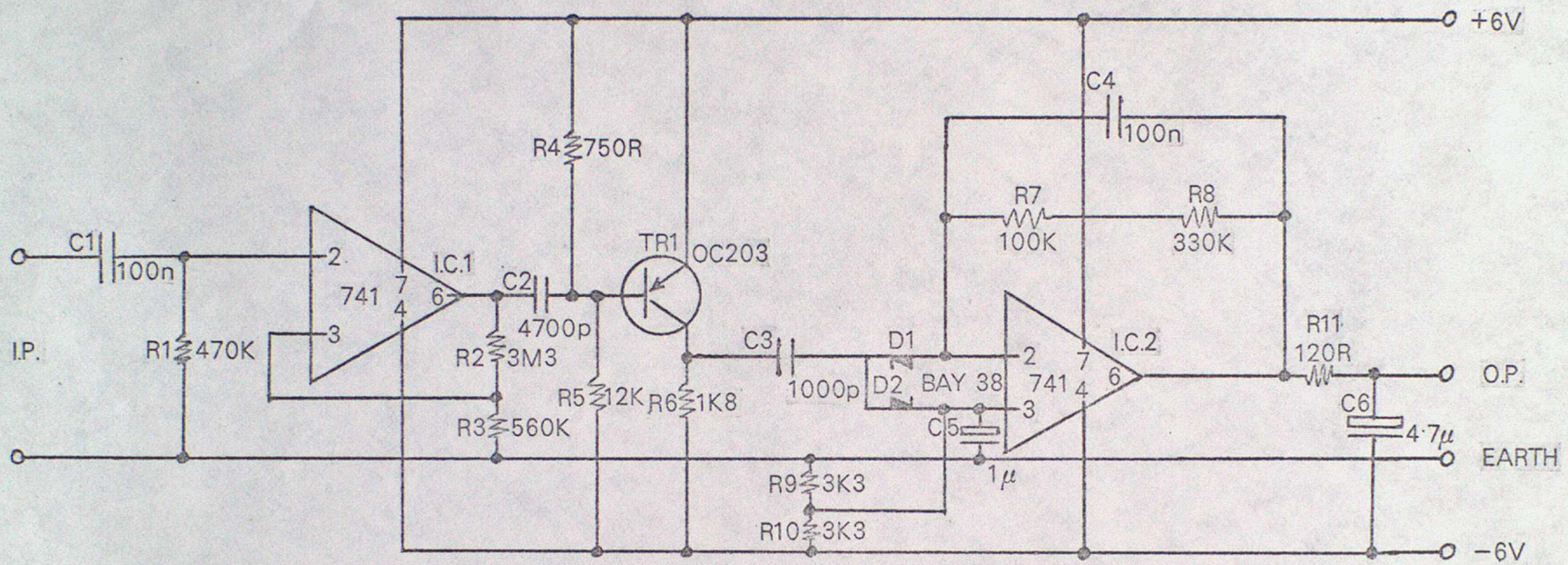
+6V
C4
100n
R4 750R
R7
100K
R8
330K
C1
100n
I.P.
R1 470K
I.C.1
741
2
3
7
4
6
C2
4700p
R2 3M3
R3 560K
R5 12K
R6 1K8
TR1 OC203
C3
1000p
D1
D2 BAY 38
C5
1μ
I.C.2
741
2
3
7
4
6
R11
120R
C6
4·7μ
O.P.
EARTH
R9 3K3
R10 3K3
−6V

DIAGRAM 4.

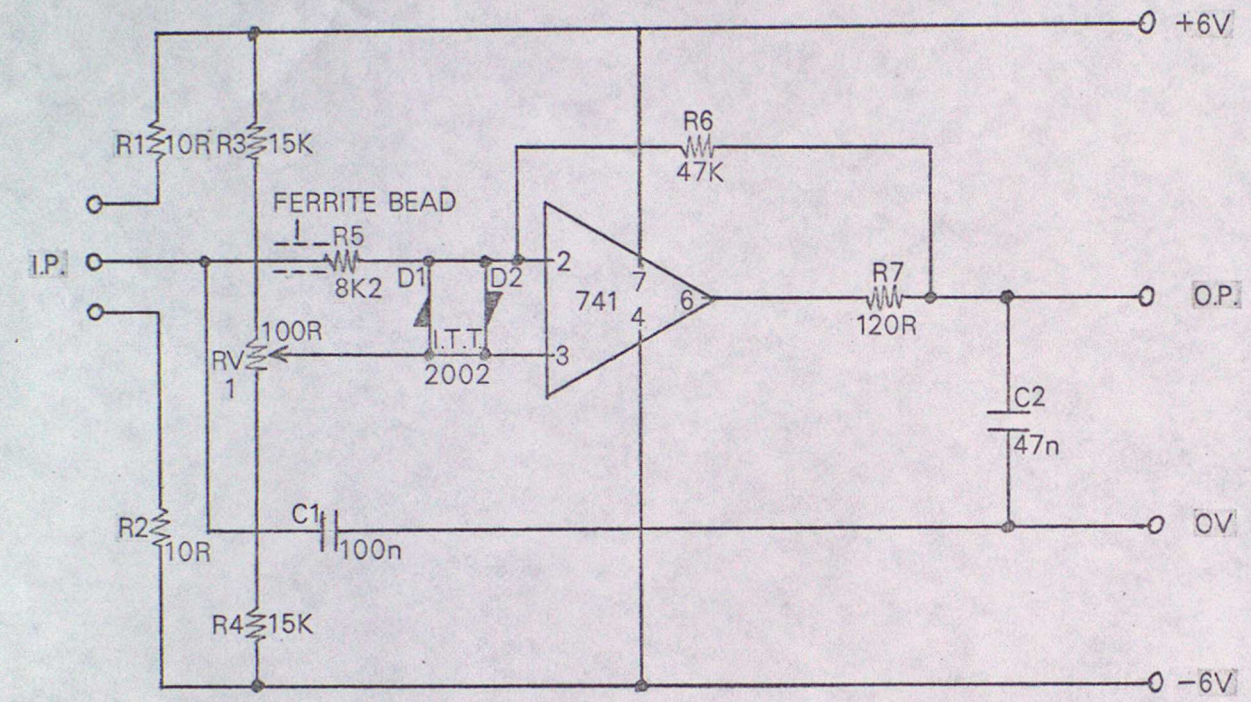

DIAGRAM 5B.

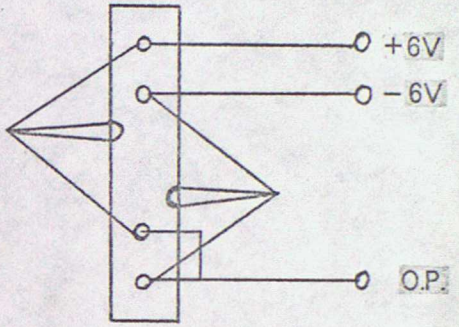

DIAGRAM 5A.

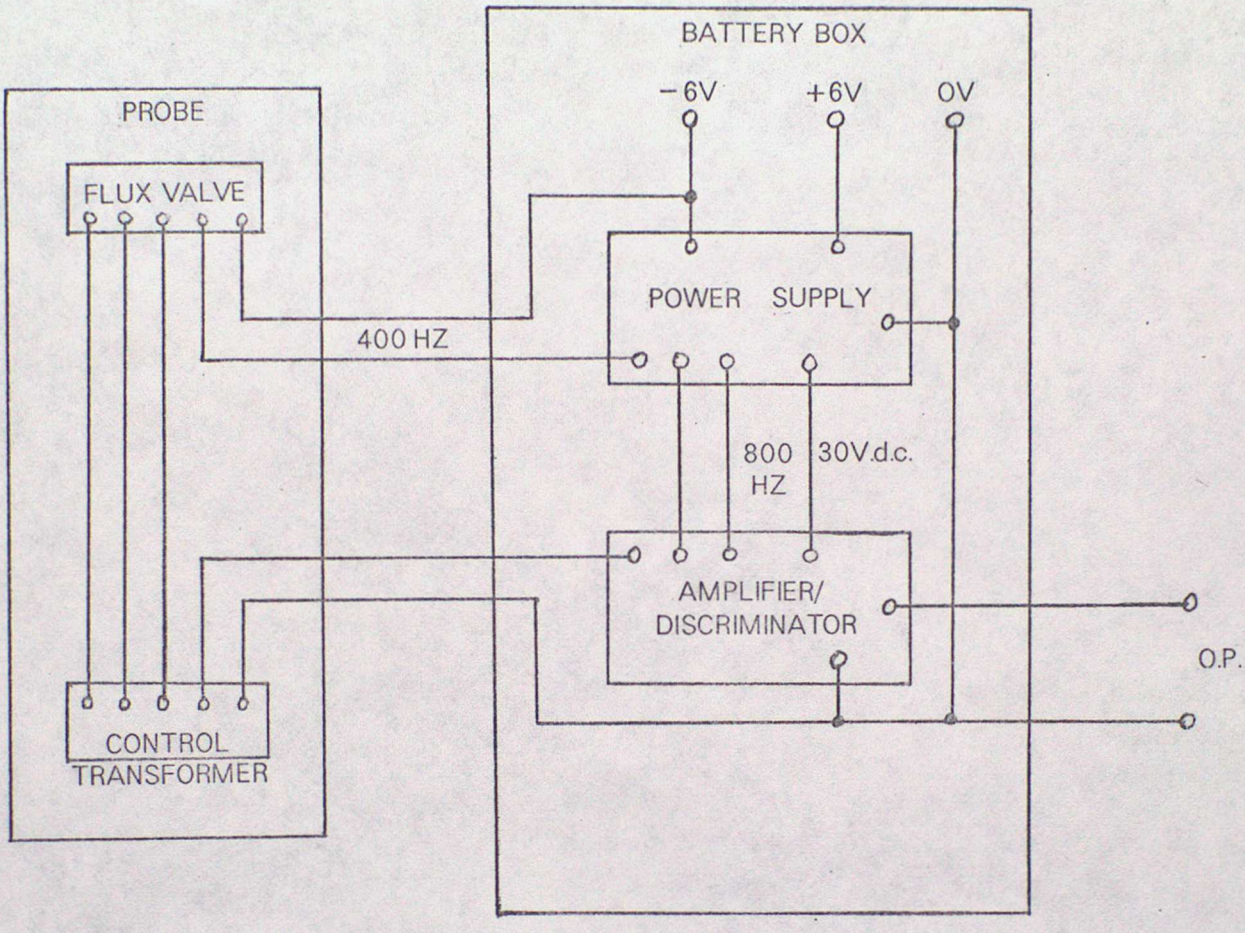
BATTERY BOX
−6V
+6V
0V
PROBE
FLUX VALVE
POWER SUPPLY
400 HZ
800 HZ
30V.d.c.
AMPLIFIER/ DISCRIMINATOR
O.P.
CONTROL TRANSFORMER

DIAGRAM 6.

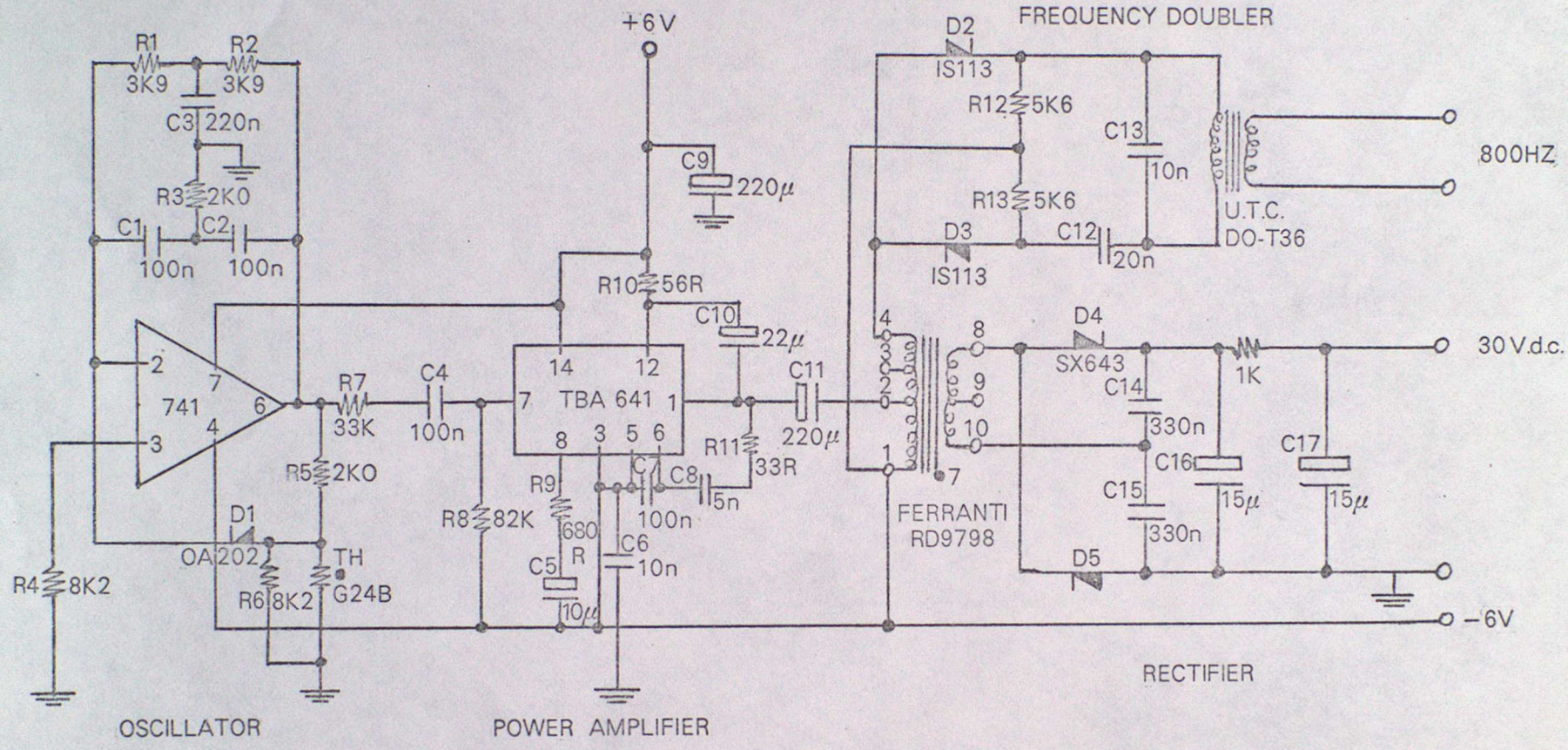
+6V
FREQUENCY DOUBLER
D2
IS113
R1
3K9
R2
3K9
C3 220n
R3 2K0
C1
100n
C2
100n
C9
220µ
R12 5K6
C13
10n
R13 5K6
D3
IS113
C12
20n
U.T.C.
DO-T36
800HZ
R10 56R
C10
22µ
D4
SX643
30 V.d.c.
1K
C14
330n
C16
15µ
C17
15µ
C15
330n
D5
741
R7
33K
C4
100n
TBA 641
C11
220µ
R11
33R
C7
100n
C8
5n
R5 2KO
R9
680
R
C5
10µ
C6
10n
R8 82K
D1
OA 202
TH
G24B
R6 8K2
R4 8K2
FERRANTI
RD9798
−6V
RECTIFIER
OSCILLATOR
POWER AMPLIFIER

DIAGRAM 7.

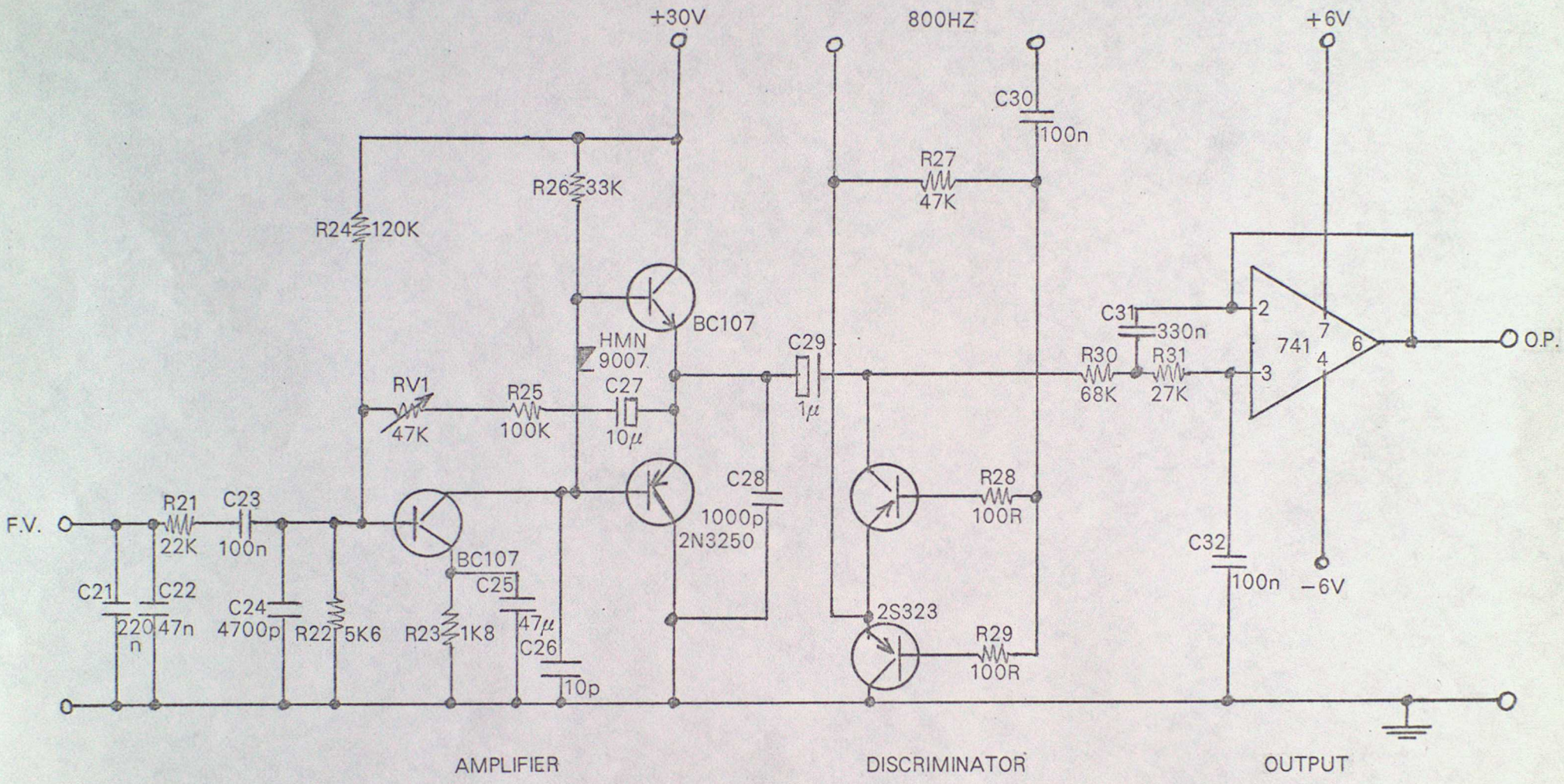
+30V
800HZ
+6V
C30
100n
R27
47K
R26 33K
R24 120K
BC107
HMN
9007
C29
1μ
C31
330n
R30
68K
R31
27K
741
O.P.
RV1
47K
R25
100K
C27
10μ
C28
1000p
2N3250
R28
100R
F.V.
R21
22K
C23
100n
BC107
C25
47μ
C26
10p
C21
220n
C22
47n
C24
4700p
R22 5K6
R23 1K8
2S323
R29
100R
C32
100n
-6V
AMPLIFIER
DISCRIMINATOR
OUTPUT

DIAGRAM 8.

E.R.

Figure 9

The results of the 1970 comparison of two turbulence - probes at Cardington. a) comparison of the standard deviations.

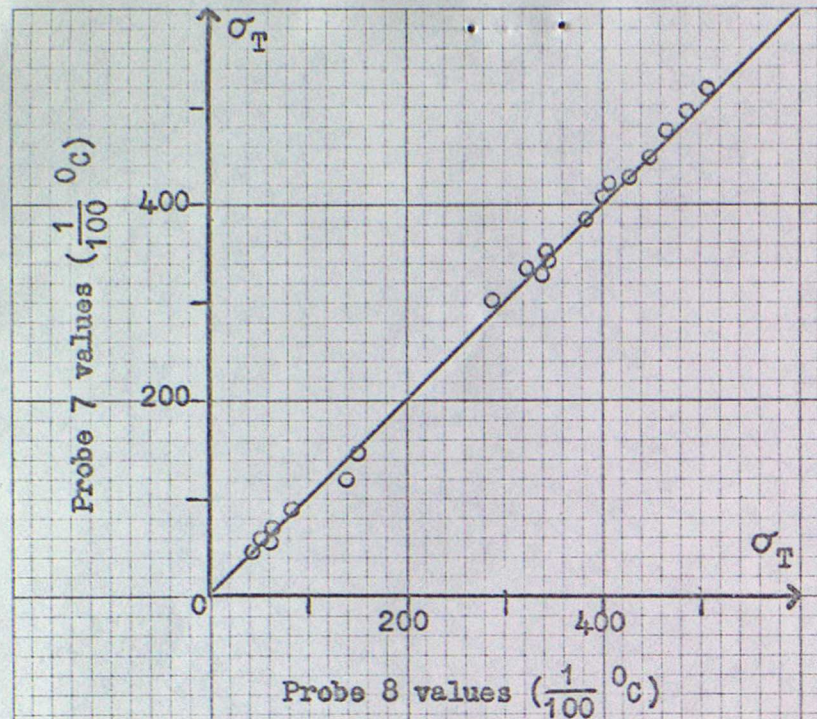

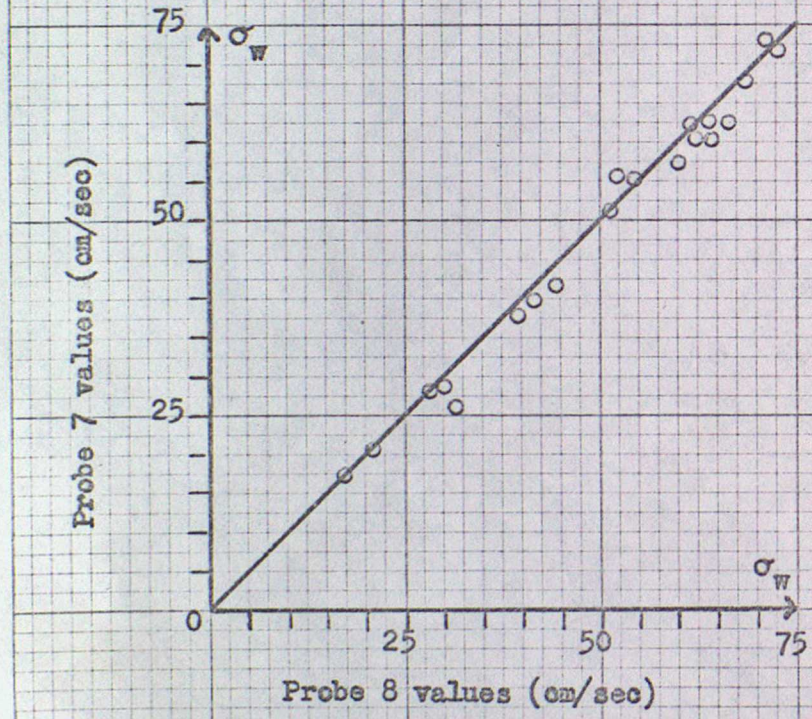

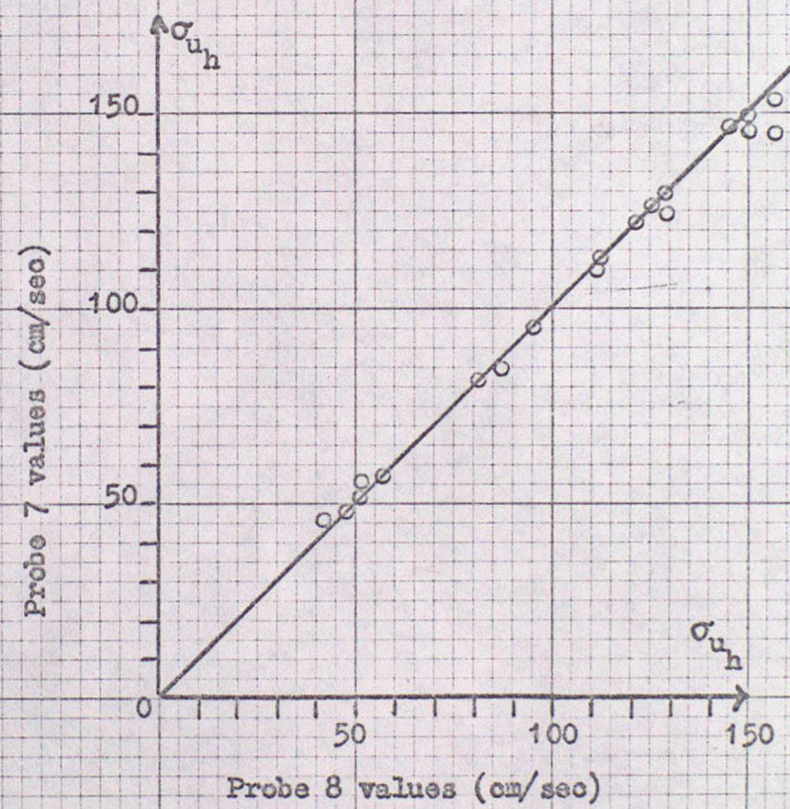

E.R.

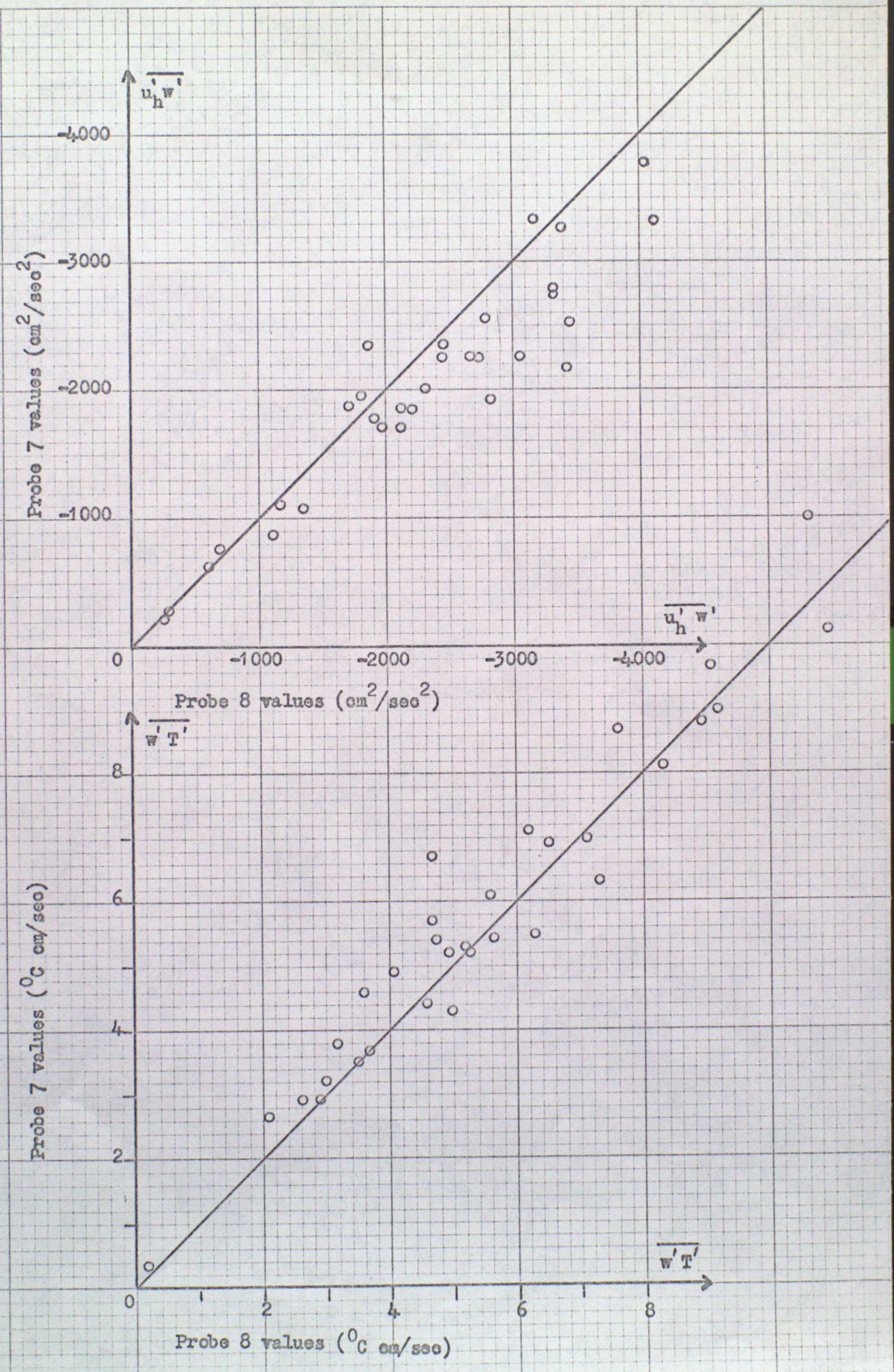

Figure 10 Comparison of the fluxes

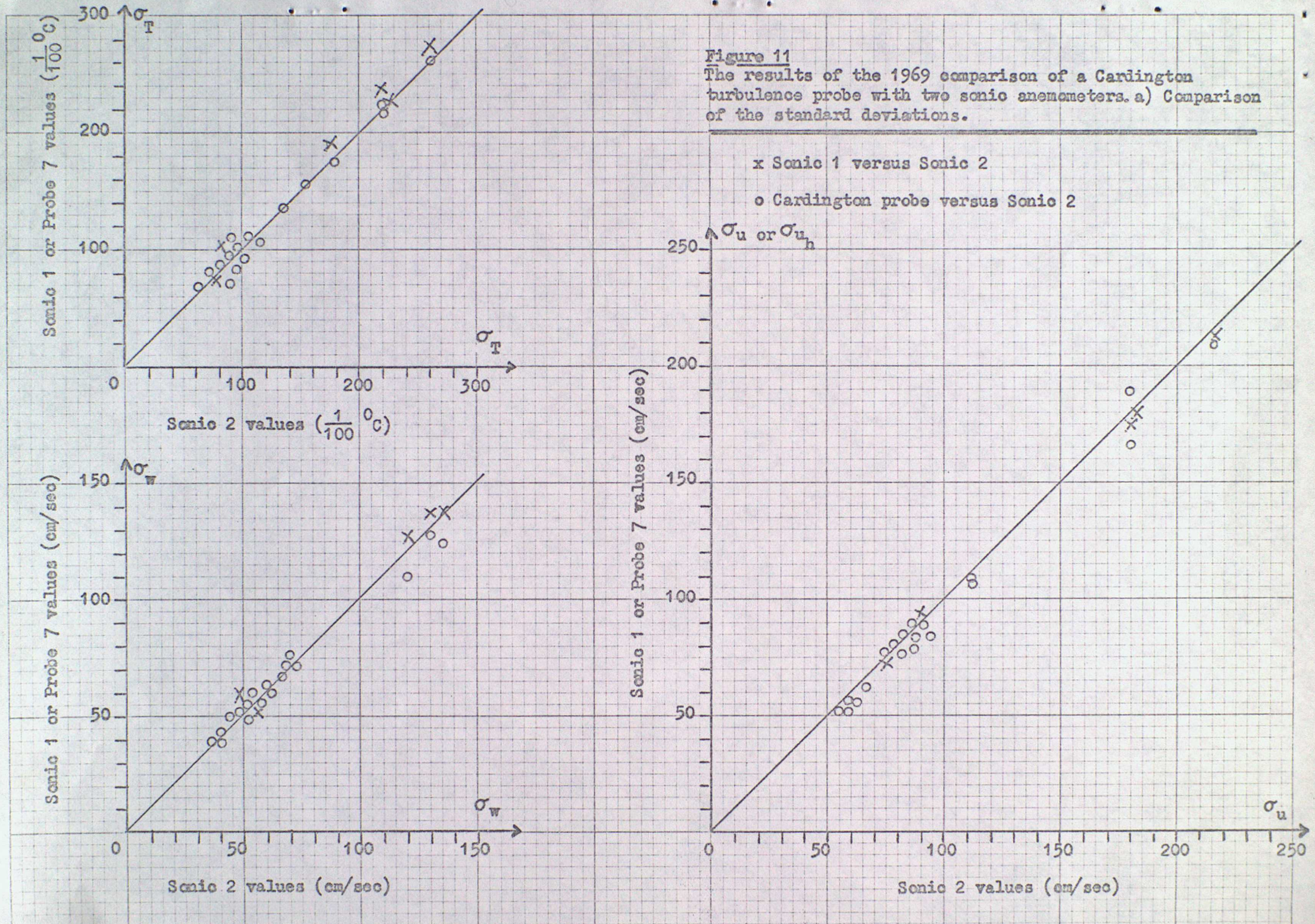

Figure 11
The results of the 1969 comparison of a Cardington turbulence probe with two sonic anemometers. a) Comparison of the standard deviations.

x Sonic 1 versus Sonic 2

o Cardington probe versus Sonic 2

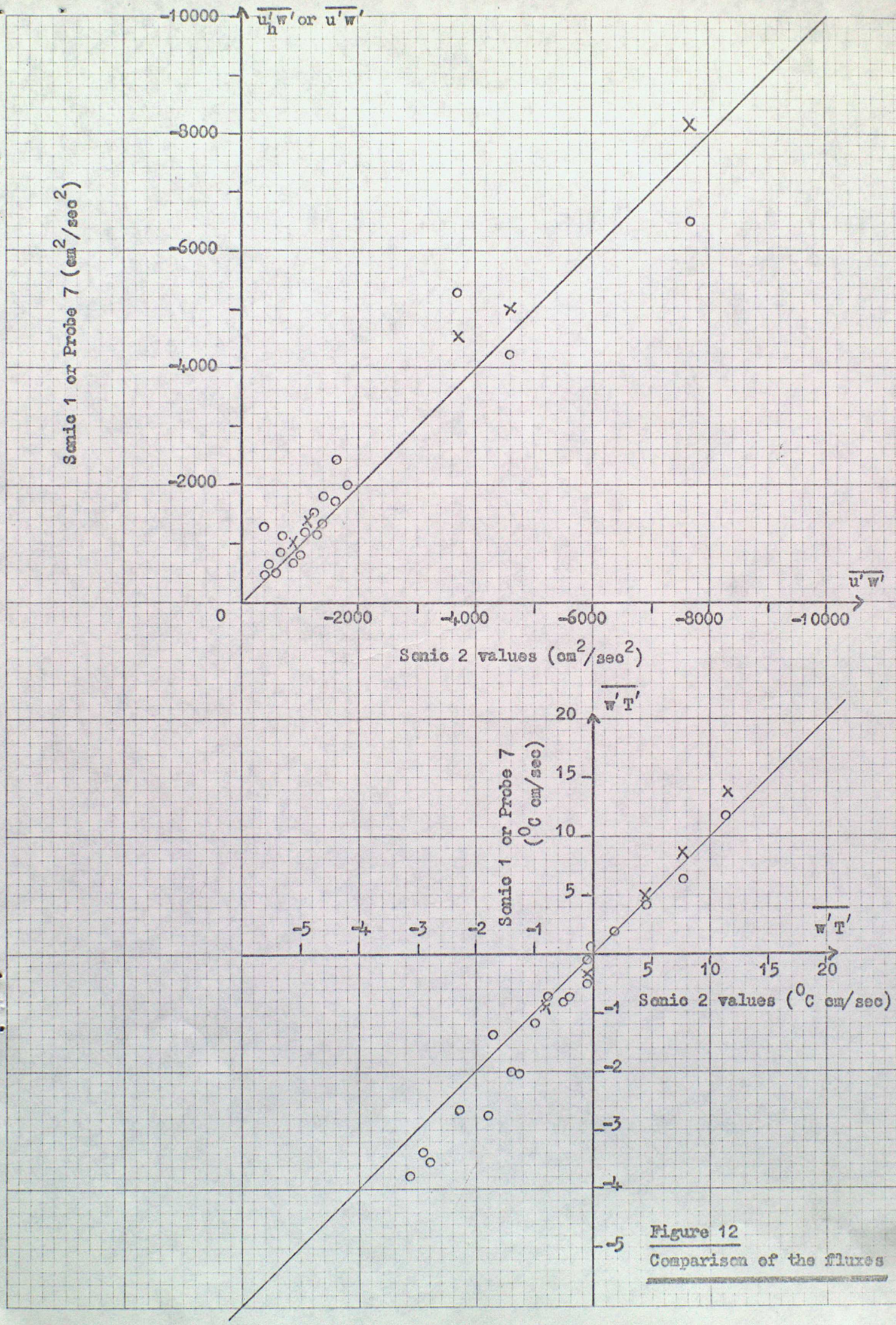

Figure 12

Comparison of the fluxes

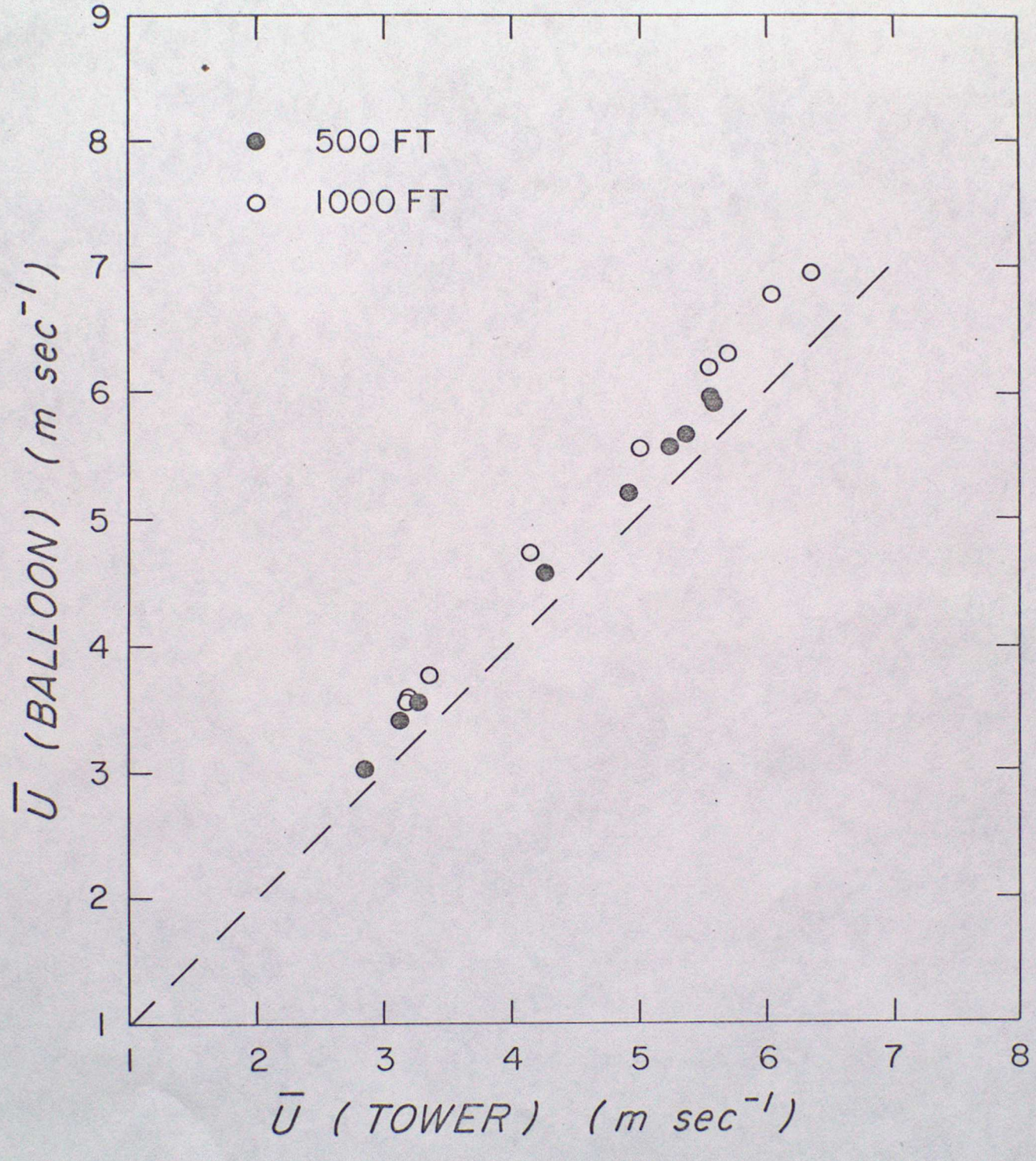
500 FT
1000 FT
$\bar{U}$ (BALLOON) (m sec^{-1})
$\bar{U}$ (TOWER) (m sec^{-1})
1
2
3
4
5
6
7
8
9

Figure 13

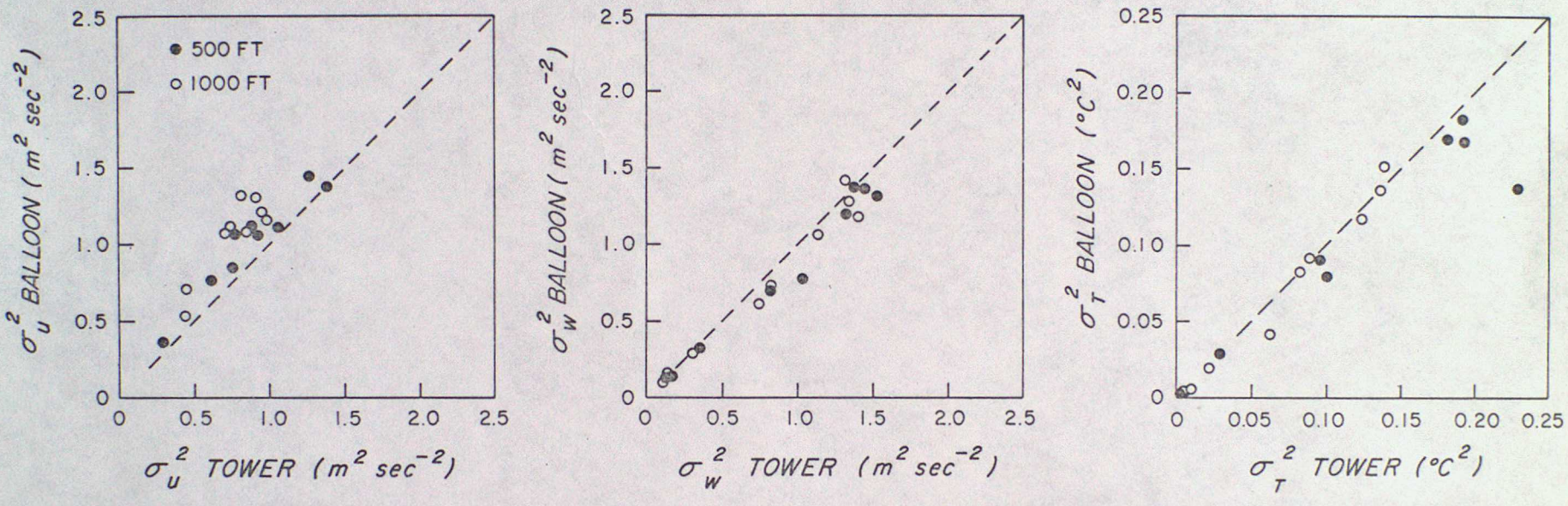

Figure 14

AFCRL PHOTO 63-63

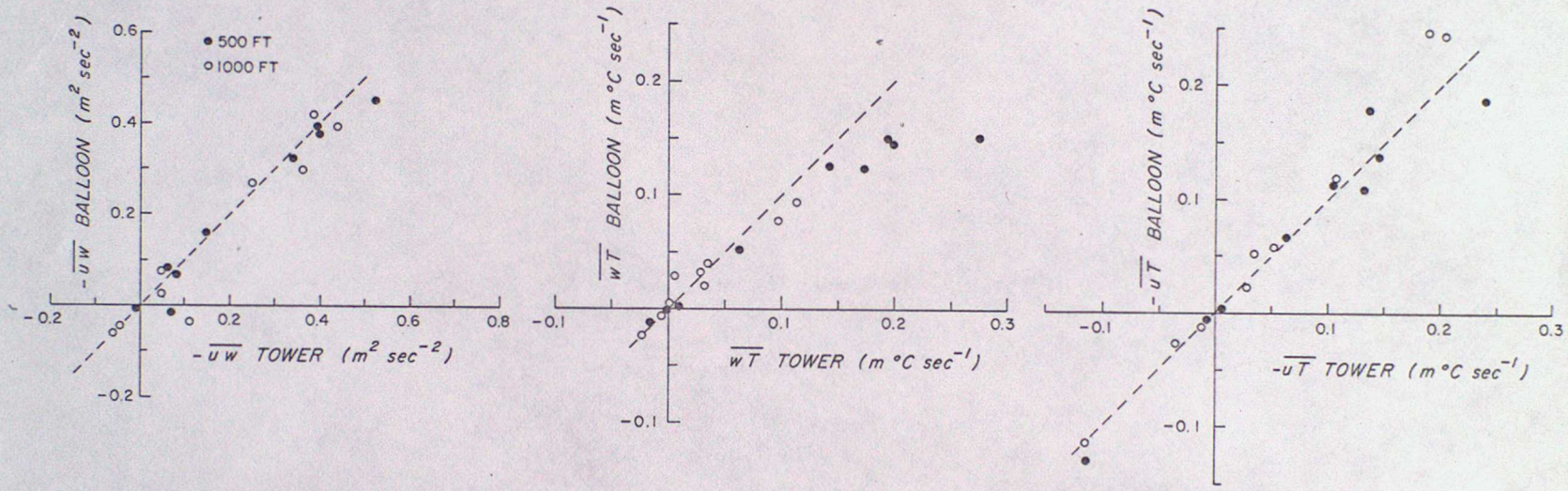
● 500 FT
○ 1000 FT
$-\overline{uw}$ BALLOON ($m^2\ sec^{-2}$)
$-\overline{uw}$ TOWER ($m^2\ sec^{-2}$)
$\overline{wT}$ BALLOON ($m\ °C\ sec^{-1}$)
$\overline{wT}$ TOWER ($m\ °C\ sec^{-1}$)
$-\overline{uT}$ BALLOON ($m\ °C\ sec^{-1}$)
$-\overline{uT}$ TOWER ($m\ °C\ sec^{-1}$)

Figure 15

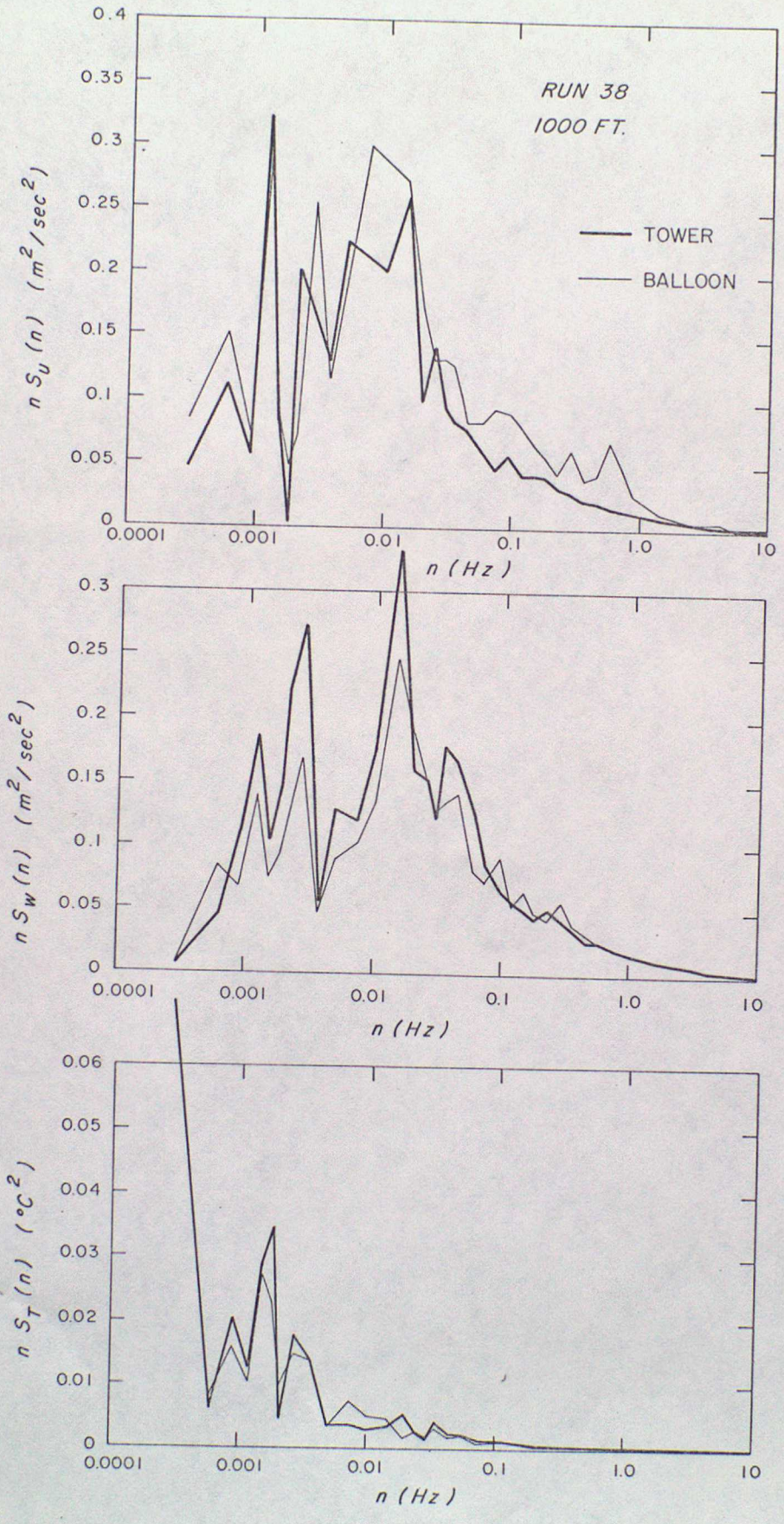
RUN 38
1000 FT.
TOWER
BALLOON
n S_U (n) (m²/sec²)
n S_W (n) (m²/sec²)
n S_T (n) (°C²)
n (Hz)
0.0001
0.001
0.01
0.1
1.0
10

Figure 16

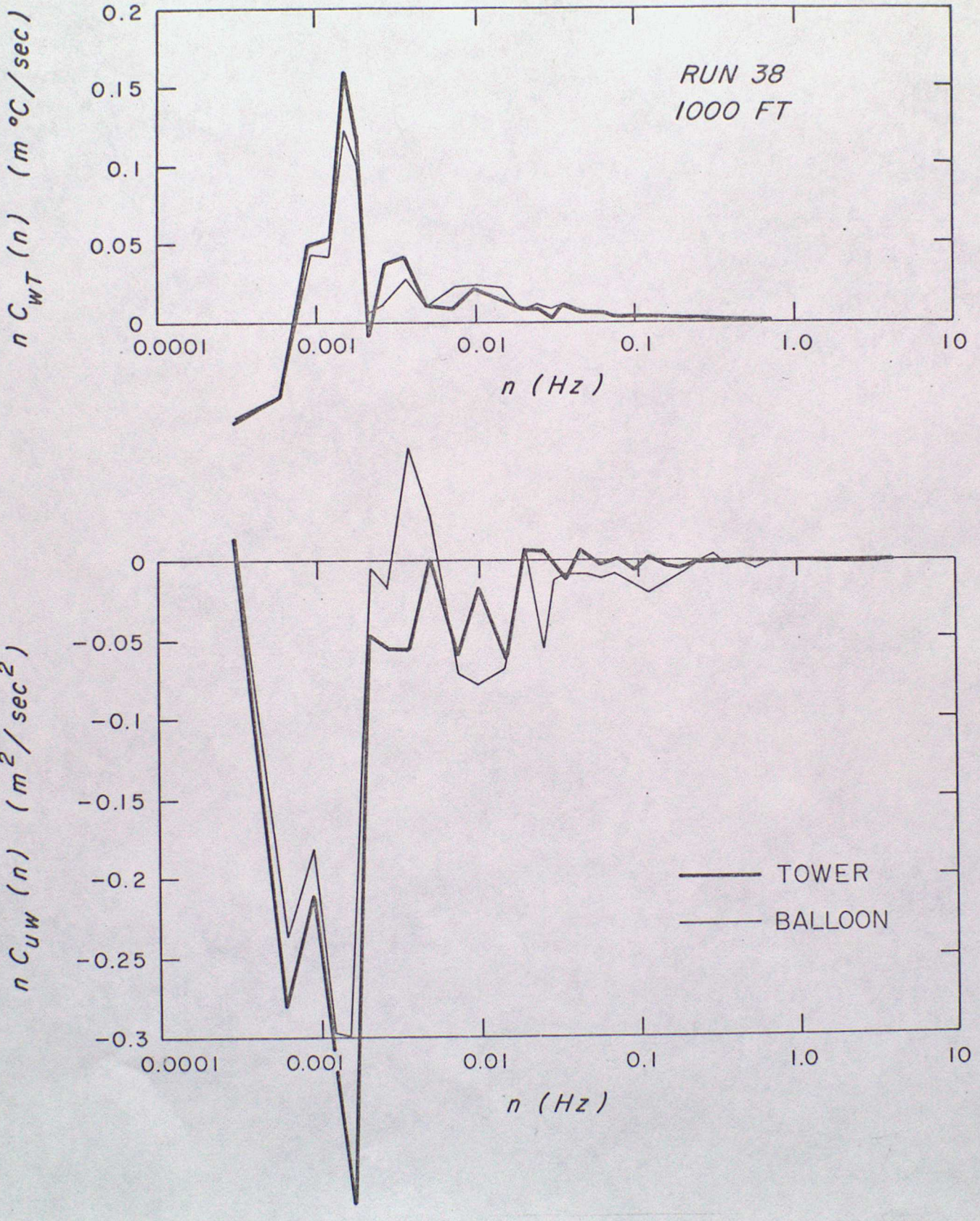
RUN 38
1000 FT
0.2
0.15
0.1
0.05
0
0.0001
0.001
0.01
0.1
1.0
10
n (Hz)
n C_WT (n) (m °C/sec)
0
-0.05
-0.1
-0.15
-0.2
-0.25
-0.3
TOWER
BALLOON
n C_uw (n) (m²/sec²)

Figure 17

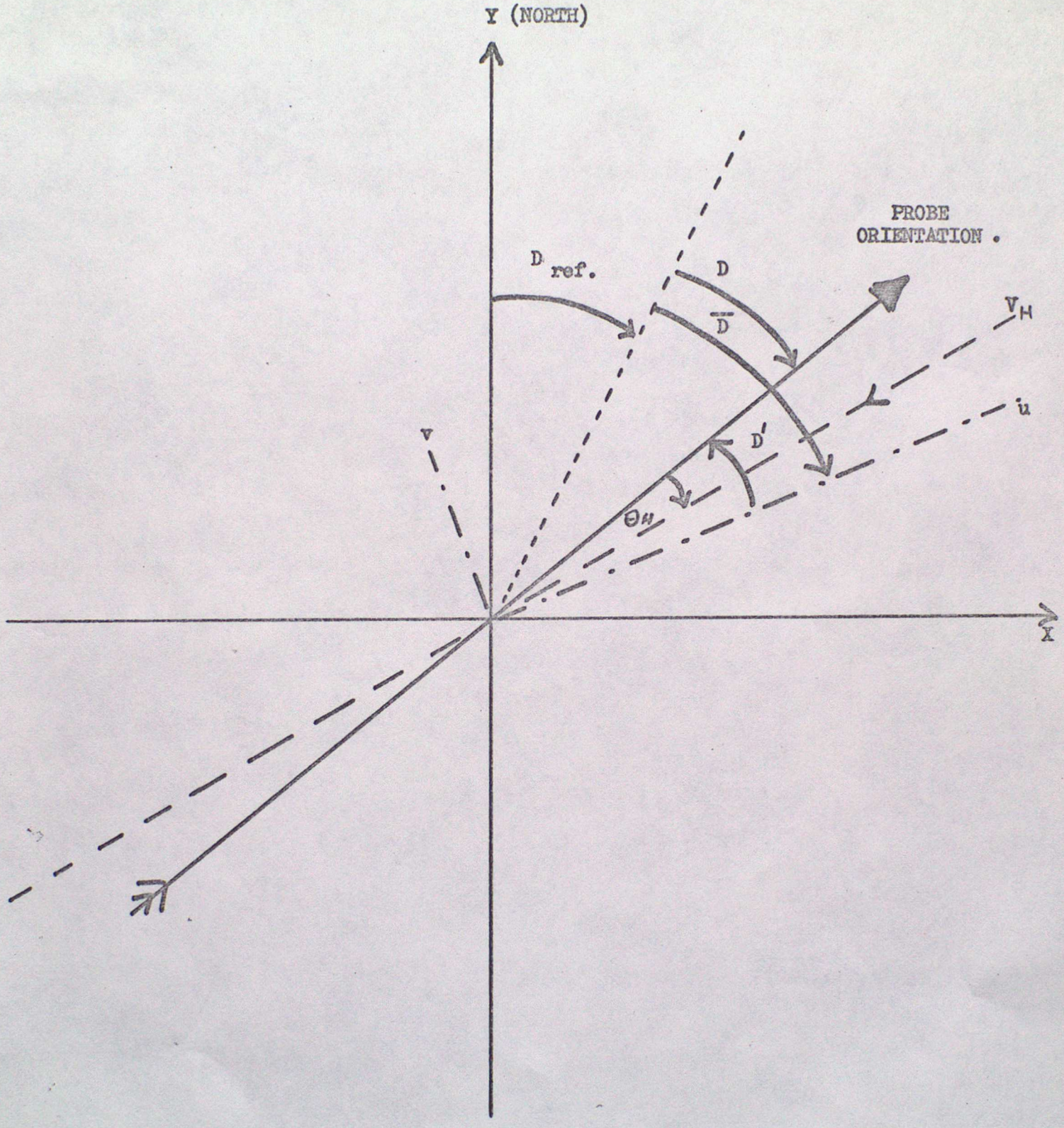

The u direction is given essentially by $\overline{D}$ and $D_{ref.}$

Figure 18